Mediator kinase inhibition suppresses hyperactive interferon signaling in Down syndrome

Kira Cozzolino[1]; Lynn Sanford[2,3]; Samuel Hunter[2,3]; Kayla Molison[1]; Benjamin Erickson[4,5]; Taylor Jones[1]; Deepa Ajit[6]; Matthew D. Galbraith[7,8]; Joaquin M. Espinosa[7,8]; David L. Bentley[4,5]; Mary A. Allen[2,3]; Robin D. Dowell[2,3]; Dylan J. Taatjes[1]*§

[1]Dept. of Biochemistry, University of Colorado, Boulder, CO, 80303, USA
[2]Dept. of Molecular, Cellular, and Developmental Biology, University of Colorado, Boulder, CO, 80303, USA
[3]BioFrontiers Institute, University of Colorado, Boulder, CO, 80303, USA
[4]Dept. Biochemistry and Molecular Genetics, University of Colorado School of Medicine, Aurora, CO 80045, USA.
[5]UC-Denver RNA Bioscience Initiative
[6]Metabolon, Inc., Durham, North Carolina, USA.
[7]Dept. of Pharmacology, University of Colorado Anschutz Medical Campus, Aurora, CO 80045, USA
[8]Linda Crnic Institute for Down Syndrome, University of Colorado Anschutz Medical Campus, Aurora, CO 80045, USA

*corresponding author
§Lead contact
email: taatjes@colorado.edu

Abstract

Hyperactive interferon (IFN) signaling is a hallmark of Down syndrome (DS), a condition caused by trisomy 21 (T21); strategies that normalize IFN signaling could benefit this population. Mediator-associated kinases CDK8 and CDK19 drive inflammatory responses through incompletely understood mechanisms. Using sibling-matched cell lines with/without T21, we investigated Mediator kinase function in the context of hyperactive IFN in DS. Using both targeted and unbiased, discovery-based approaches, we identified new and diverse mechanisms by which Mediator kinases regulate IFN signaling. Beyond effects on IFN-stimulated transcripts, we discovered that CDK8/CDK19 impact splicing, revealing a novel means by which Mediator kinases control gene expression. Kinase inhibition altered splicing in pathway-specific ways and selectively disrupted IFN-responsive gene splicing in T21 cells. Moreover, Mediator kinase inhibition blocked cytokine responses to IFNγ and severely impacted core metabolic pathways, including up-regulation of anti-inflammatory lipid signaling molecules during IFNγ-stimulation. These lipids included ligands for nuclear receptors and G-protein coupled receptors that can act in an autocrine or paracrine manner, suggesting additional kinase-dependent mechanisms to durably suppress IFNγ responses, beyond initial changes in gene expression. Collectively, our results establish that Mediator kinase inhibition antagonizes IFNγ signaling through transcriptional, metabolic, and cytokine responses, with implications for DS and other chronic inflammatory conditions.

Significance

As Mediator-associated kinases, CDK8 and CDK19 are established regulators of RNA polymerase II transcription; however, the "downstream" biochemical impacts of CDK8/CDK19 inhibition have not been thoroughly examined. We previously showed that CDK8 and CDK19 help activate transcriptional responses to the universal cytokine IFNγ; others have demonstrated that Down syndrome (DS) is characterized by hyperactive IFNγ signaling, which contributes to DS-associated

pathologies. Here, we discovered CDK8/CDK19 inhibition drives "downstream" metabolic changes that can reinforce and propagate anti-inflammatory responses independent of transcription. We also identified a new means by which CDK8/CDK19 regulate gene expression, via alternative splicing, and inhibition selectively impacted IFNγ response genes. Collectively, our results establish that Mediator kinase inhibition antagonizes hyperactive IFN signaling in DS, suggesting novel therapeutic strategies.

Introduction

Down syndrome (DS) is relatively common in the human population (ca. 1 in 700 live births)(1) and results from trisomy of chromosome 21 (T21). T21 manifests in myriad ways, including an increased propensity for autoimmune and neurological disorders, as well as elevated incidence of leukemia (2-4). Notably, T21 also results in chronic immune dysregulation associated with hyperactivation of interferon (IFN) signaling (5-7).

The chronic, hyperactive IFN response in DS can be attributed, at least in part, to the fact that four IFN receptors are encoded on chromosome 21: IFNAR1 and IFNAR2 for Type I IFNs (e.g., IFNβ, IFNγ), IFNGR2 for IFNγ, and the Type III subunit IL10RB for IFNλ, which also serves as a subunit of the IL10 receptor. Numerous pathologies associated with DS, including autoimmune-related disorders, are considered direct consequences of chronic IFN pathway activation (5, 7-10). For these and other reasons, hyperactive IFN signaling lies at the heart of DS pathophysiology (11), and therapeutic strategies to dampen IFN responses are already being tested in clinical trials for multiple clinicial endpoints in DS (NCT04246372, NCT05662228).

We recently demonstrated that the Mediator kinases (CDK8 and its paralog CDK19) are important drivers of inflammatory responses to the universal cytokine IFNγ (12). This discovery has implications for DS, not only because of IFN signaling, but also because Mediator kinases represent viable targets for molecular therapeutics, in part due to low toxicity of a selective inhibitor in mouse models (13). Many studies have linked Mediator kinase activity to immune system function and inflammatory responses (12, 14-20), and CDK8/CDK19 inhibition can suppress autoimmune disease in animal models (21). Mediator kinases target the STAT transcription factor (TF) family (14, 22) and activation of JAK/STAT pathway TFs (e.g. STAT1, IRF1) is blocked upon Mediator kinase inhibition in human and mouse cells (12). Collectively, these results suggest that Mediator kinase activity could contribute to IFN signaling in T21 cells, and that Mediator kinase inhibition could mitigate chronic, hyperactive IFN signaling in T21.

Mediator is a 26-subunit complex that regulates RNA polymerase II (RNAPII) transcription genome-wide (23). Mediator is recruited to specific genomic loci through interactions with sequence-specific, DNA-binding TFs, and Mediator also interacts extensively with the RNAPII enzyme at transcription start sites. Through these distinct interactions, Mediator enables TF-dependent control of RNAPII function. CDK8 or CDK19 can reversibly associate with Mediator as part of a 4-subunit "Mediator kinase module" that contains additional subunits MED12, MED13, and CCNC (24).

Mediator kinases have not been studied in the context of DS, and a goal of this project was to define their roles in the context of IFNγ signaling, using donor-derived cell lines. We also sought to address other fundamental questions regarding Mediator kinase function that remained largely unexplored. For instance, it is not known whether Mediator kinases impact pre-mRNA splicing that is coupled to RNAPII transcription, despite evidence that CDK8 and/or CDK19 phosphorylate splicing regulatory proteins (22). Furthermore, metabolic changes are at least as important as transcriptional changes in driving biological responses (25, 26), but how Mediator kinases impact metabolism in human cells remains incompletely understood (27, 28). Finally, cytokines serve as

2

key drivers of cellular IFNγ responses, and despite links between CDK8/CDK19 function and inflammation (12, 15, 16), it is largely unknown how Mediator kinases might impact cytokine levels.

Using a combination of approaches, we have identified novel and diverse mechanisms by which Mediator kinases control IFNγ responses under both basal and IFNγ-stimulated conditions. Beyond anticipated effects on RNAPII transcription, we discovered that Mediator kinases selectively control gene expression through pre-mRNA splicing, and that regulation of cytokine and metabolite levels contributes to CDK8/CDK19-dependent control of pro-inflammatory IFNγ signaling. Taken together, these and other results identify Mediator kinases as therapeutic targets that could mitigate immune system dysregulation in individuals with DS.

Results
Experimental overview: transcriptomics, metabolomics, and cytokine screens
The basic goals of this project were to compare and contrast transcriptional and metabolic changes in the following experimental contexts: i) T21 vs. D21, ii) ±IFNγ stimulation, iii) ±Mediator kinase inhibition, and iv) IFNγ stimulation + Mediator kinase inhibition. For T21 vs. D21 comparisons, we selected lymphoblastoid cells from the Nexus Biobank that were derived from siblings matched in age (3- or 5-year old) and sex (male). Unless otherwise noted, these lines were used for all analyses described herein. We used the natural product cortistatin A (CA) to inhibit CDK8 and CDK19 (13). CA is the most potent and selective Mediator kinase inhibitor available (29); for example, kinome-wide screens showed no off-target kinase inhibition even at 1 μM, which is a concentration 5000-times greater than its measured K_D of 0.2 nM (13). Throughout this project, we used CA at a concentration of 100 nM.

Prior to completion of RNA-seq experiments, we probed the timing of the IFNγ response at IFN target genes GBP1 and IRF1 with RT-qPCR (**Fig S1A**). Based upon these results, we chose the 4-hour time point for RNA-seq (see Methods). An overview of the RNA-seq experiments is shown in **Figure 1A**, with data for all genes across all conditions in **Table S1**.

Large-scale, untargeted metabolomic analyses were completed 24h post-IFNγ stimulation in D21 and T21 cells. This time point was chosen to approximate a "steady state" following IFNγ treatment and to allow time for metabolic adaptations to occur; this time point was also consistent with prior metabolite analyses in IFN-treated cells (30, 31). Moreover, the 24h time point would complement the 4h RNA-seq data, in that transcriptional changes identified at 4h might contribute to subsequent metabolic changes. An overview of the metabolomics experiments is shown in **Figure 1A**, with raw data for all identified metabolites across conditions in **Table S2**.

Down syndrome has been described as a "cytokinopathy" based upon evaluation of plasma from individuals with or without T21. Arrays screening 29 different cytokines showed elevated levels in Down syndrome individuals (32). Based upon these and other results, we sought to directly measure cytokine levels to assess IFNγ and CA-dependent effects. Therefore, we completed a series of cytokine screens (n=105 different cytokines) in T21 and D21 cells, using the same experimental design as the metabolomics experiments (basal conditions, +CA, +IFNγ, or +CA+IFNγ). Biological replicate cytokine screens were completed for each condition after 24h treatment; measurements for all cytokines in both replicates with ANOVA p-values can be found in **Table S3**. As expected, not all 105 cytokines were detected at significant levels in D21 and T21 cells and many cytokines were shared in each cell line (**Fig S1B**).

The T21 transcriptome, metabolome, and cytokine levels are consistent with hyperactive IFN signaling
For RNA-seq, biological triplicate experiments were completed, and a normalization (33) was performed to account for the potential 1.5-fold expression differences from chromosome 21 in T21

3

cells (34). Comparison of gene expression in T21 vs. D21 cells revealed massive differences, as expected (**Fig S1C, Table S1**). Gene set enrichment analysis (GSEA)(35) based upon the T21 vs. D21 RNA-seq results revealed enrichment of inflammatory pathways (e.g. IFNγ, IFNα, Complement, TNFα) in T21 cells (**Fig S1D, Table S4**), consistent with prior reports (6, 32, 36). Furthermore, the "upstream regulators" identified from Ingenuity Pathway Analysis (IPA) (37) predicted activation of numerous inflammatory markers in T21 cells (e.g. IFNγ, IFNα, TNF, TGFβ1, NFκB) based upon the RNA-seq results (**Fig S1E, Table S5**). Negatively enriched pathways in T21 cells (GSEA Hallmarks, **Fig S1D, Table S4**) reflected proliferative gene expression programs (e.g. MYC targets, G2M checkpoint); in agreement, we observed slower growth rates for T21 cells compared with their D21 counterparts. We also characterized T21-specific differences in splicing, which will be described later.

Untargeted metabolomics experiments identified and quantified over 600 biochemicals representing every major metabolic pathway (**Table S2**). We observed widespread differences between T21 and D21 cells (**Fig S1F, G; Table S2**), with evidence that inflammatory pathways were basally activated in T21 cells (IPA results, **Fig S1H, Table S5**), whereas pathways related to fatty acid transport, growth, and energy metabolism were reduced (vs. D21; **Fig S1H**). Supporting these general trends, the metabolomics data revealed T21-specific changes in glycolysis, nucleotide and lipid biosynthesis, and other fundamental cellular processes (**Fig S1G; Table S2**). Metabolic distinctions between T21 and D21 cells will be described in more detail later, in the context of IFNγ treatment and/or Mediator kinase inhibition. An overview of metabolic pathways that are relevant for this study is shown in **Figure 1B**.

As with the RNA-seq and metabolomics data, the cytokine screen results implicated chronic activation of the IFN response in T21 cells under basal conditions; for example, levels of many cytokines were elevated in T21 vs. D21 cells under basal conditions (**Fig 1C**, left column). Furthermore, treatment with IFNγ appeared to "normalize" cytokine levels in T21 vs. D21 cells (**Fig 1C**, right column), such that many cytokines were detected at roughly equal levels in IFNγ-stimulated T21 and D21 cells.

T21-specific transcriptional, metabolic, and cytokine changes are reflected in population-level data

For practical reasons, the in-depth transcriptomics, metabolomics, and cytokine screening experiments completed here precluded parallel examination of additional genetically distinct donor-derived T21 and D21 cell lines. A basic observation from past studies was that the transcriptomes of T21 individuals are not only tissue- and cell type-specific, but also reflect individual-to-individual differences within the same cell types (6, 34). However, we hypothesized that the general trends in our sibling-matched T21 vs. D21 lines would show some commonality with data from large-scale cohort studies.

We analyzed RNA-seq data from whole blood samples from individuals with DS (n=304) or euploid (i.e. D21; n=96) controls (11), generated by the Human Trisome Project (www.trisome.org, NCT02864108). The data revealed upregulation of the IFNγ response, Complement, cytokine production, and other inflammatory pathways in T21 individuals (vs. D21; **Fig. S2A; Table S4**). Approximately ten percent of differentially expressed genes were shared between the Human Trisome Project cohort study (T21 vs. D21; whole blood transcriptomes from individuals varying in age and sex) and our RNA-seq results from sibling-matched T21 and D21 lymphoblastoid cell lines (**Fig S2B**), consistent with individual-to-individual variation within the human population (6, 34). However, the shared "core sets" of genes reflected prominent trends in our T21/D21 RNA-seq comparisons. For example, up-regulated genes represented cytokine production and other inflammatory pathways, whereas down-regulated genes involved nucleotide metabolism, splicing,

GPCR signaling, and proliferation. These pathway trends are well-represented in our RNA-seq and metabolomics data (e.g. **Fig S1D, H; Table S6**) and additional data supporting these T21-specific alterations will be described in more detail later.

A recent analysis of blood plasma cytokine levels, measuring 29 cytokines from DS individuals (n=21) or age-matched euploid controls (n=10) identified elevated levels of approximately 10 to as many as 22 of these cytokines (32). In agreement, at least 13 of these 22 cytokines (59%) were elevated in our T21 vs. D21 comparison (red font in **Fig 1C**). Collectively, the RNA-seq and cytokine data from cohorts of DS individuals indicate that the two model cell lines evaluated here, derived from age- and sibling-matched D21 and T21 individuals, broadly reflect population-wide trends.

Mediator kinase inhibition tempers T21 inflammatory pathways under basal conditions

Collectively, the RNA-seq, metabolomics, and cytokine data from sibling-matched T21 or D21 individuals showed evidence for chronic inflammatory signaling in T21 cells, consistent with prior reports (6, 32, 38-40). Whereas these results provided assurances about our cell line models, we were most interested to determine how or whether Mediator kinases influence inflammatory signaling and IFNγ responses in T21 and D21 cells. Therefore, we compared the transcriptional, metabolic, and cytokine responses to IFNγ and/or CA in T21 and D21 cells. We first describe how Mediator kinase inhibition impacted T21 or D21 cells under basal conditions.

Transcriptome: As shown in **Figure 2A, Figure S3A-D,** and **Table S4**, CA caused similar changes to gene expression programs in T21 and D21 cells, although some T21-specific differences were evident (**Fig S3C, D**). GSEA showed downregulation of MYC targets, consistent with prior studies in CDK8-depleted cells (41). Downregulation of the inflammatory "TNFα signaling via NFκB" pathway was also observed in CA-treated D21 and T21 cells (**Fig S3C, D**); decreased expression of the NFKB1 and NFKB2 transcripts themselves likely contributed to this effect (**Table S1**). Regulation of NFκB transcriptional programs has been previously linked to the Mediator kinases (15) although direct control of NFκB transcription levels has not been reported. Activation of GSEA Hallmarks related to mTOR signaling, cholesterol and fatty acid metabolism were common in CA-treated D21 and T21 cells (**Fig S3C, D**), in agreement with prior studies in other cell types (22, 42, 43). To further characterize the CA-dependent transcriptional changes related to cholesterol and fatty acid metabolism, we highlighted the genes significantly up-regulated in these pathways in **Figure S3E**; the data indicate that Mediator kinases broadly regulate cholesterol and fatty acid biosynthesis, and this is further confirmed by the metabolomics data (see below).

Based upon the RNA-seq data comparing CA-treated T21 or D21 cells vs. untreated controls, we completed an "upstream regulators" analysis (IPA; **Fig S3F, Table S5**). In agreement with the GSEA results, factors regulating cholesterol homeostasis (e.g. SCAP, SREBF1/2, INSIG1), fatty acid metabolism (e.g. ACSS2, FASN), and inflammation (e.g. NFKB1, MYD88, TLR3) were identified in T21 cells (**Fig 2B; Fig S3F**), with similar results in D21 (**Fig S3F**). The IPA results also implicated CA-dependent repression of pro-inflammatory TFs specifically in T21 cells, including RELA (NFκB complex), FOXO3, and ILF3 (**Fig S3F, Table S5**), consistent with repression of chronic basal IFN signaling upon Mediator kinase inhibition. This CA-dependent effect was further supported by the metabolomic and cytokine screen data, described below.

Metabolome: CA-dependent changes in the metabolomes of D21 and T21 cells were strikingly distinct. This is likely due to i) the longer time frame used for metabolomics analyses (24h vs. 4h for RNA-seq), and ii) the massive "pre-existing" basal metabolome differences in T21 vs. D21 cells (**Table S7**). Direct comparison of T21 vs. D21 metabolomes (basal conditions) identified major differences in glycolysis, the pentose phosphate pathway, the citric acid cycle,

various categories of lipids, and nucleotide biosynthesis pathways (**Fig S1F, G**). Here, we will focus on the T21 vs. D21 metabolic differences that relate to pathways that were impacted by Mediator kinase inhibition.

In **Figure 2C**, we highlight examples of CA-dependent increases in anti-inflammatory lipid metabolites. In T21 cells selectively, CA treatment broadly increased levels of long chain mono- and poly-unsaturated FA (PUFA; **Fig 2C**), including oleic acid, eicosapentaenoate (EPA), docosapentaenoate (DPA), docosahexaenoate (DHA), and various other ω3 and ω6 PUFAs (**Table S8**). These metabolites act as signaling molecules by binding to extracellular G-protein coupled receptors (GPCRs) to trigger anti-inflammatory signaling cascades (44-47), as shown in the simplified schematic in **Figure 2D**. Similar to LCFAs, endocannabinoids were broadly elevated in CA-treated T21 cells (vs D21; **Fig 2C**). Endocannabinoids mediate anti-inflammatory effects in part through PPAR TFs (48); for example, oleoylethanolamide (OEA) is a PPARα ligand (49) that can suppress pro-inflammatory NFκB signaling (50). Collectively, these results reveal new and unexpected ways in which Mediator kinase inhibition antagonizes pro-inflammatory IFN signaling in T21.

Cytokine: CA treatment was also shown to be anti-inflammatory based upon the cytokine screen results. Under basal conditions, about two dozen cytokines responded to CA treatment (**Fig 2E**). In D21 cells, the anti-inflammatory cytokine IL10 increased upon Mediator kinase inhibition, in agreement with prior reports in other cell types (19), whereas the pro-inflammatory cytokines GMCSF, IL3, and MIP1α/β (a.k.a. CCL3/4) decreased; an exception was TNFα. Similar results were obtained in T21 cells; however, CA treatment reduced the levels of pro-inflammatory cytokines in T21 cells that were not reduced in D21 (e.g. IL32, IL33, IL34), although CXCL10 and GMCSF were exceptions. The selective CA-dependent decrease in IFNγ in T21 cells under basal conditions further supports the chronic high baseline IFN signaling in these cells (6). Note that some cytokines have regulatory roles that cannot be clearly defined as either pro- or anti-inflammatory and their roles may be cell type-specific (51).

Because cytokine levels were measured 24h after CA treatment, we hypothesized that their altered levels would at least partially correspond to gene expression changes that were measured earlier, at 4h post-treatment. Indeed, this was observed for many cytokines impacted by Mediator kinase inhibition, as shown in **Figure 2F**. (Note that expression changes for cytokine receptors are also shown.) At basal conditions, several dozen cytokines and cytokine receptors were regulated by CA at the transcriptional level (**Fig 2F**), and most correlated with the cytokine screen data, including IL10, which was transcriptionally upregulated in D21 cells, and MIP1α/β (a.k.a. CCL3/4), which were transcriptionally downregulated in both D21 and T21 lines. We also observed that CA altered the expression of two interferon receptors: IFNGR2 was downregulated and IFNAR2 was upregulated in both lines. Each of these IFN receptor genes is on chromosome 21 and associated with chronic inflammation in DS individuals (6).

Mediator kinase inhibition antagonizes IFNγ-induced transcriptional, metabolic, and cytokine responses

We next evaluated the transcriptomic, metabolomic, and cytokine data from IFNγ-treated cells. As shown in **Figure S4A**, the transcriptional response to IFNγ was broadly similar in T21 and D21 cells; however, T21 cells showed higher basal expression of inflammatory genes. This can be seen upon comparison of gene expression in T21 vs. D21 cells under basal (**Fig S4B**) or IFNγ-stimulated conditions (**Fig S4C**; see also **Fig S4D, E**). Only 10 genes showed greater expression levels in T21 cells in response to IFNγ, whereas 68 genes had reduced induction in T21 compared with D21 (**Fig S4F**). Pathway analysis (GO Biological Processes) of these 68 genes showed predominant roles in IFN signaling and inflammatory responses (**Fig S4G, Table S6**). This result is

consistent with general hyperactive IFN signaling in T21 cells (6), such that overall transcriptional induction upon exogenous IFNγ stimulation was reduced compared with D21 cells. Analogous trends were observed in cytokine levels, in which IFNγ treatment resulted in similar cytokine levels in T21 vs. D21 cells, whereas their levels were greater in unstimulated T21 cells (**Fig 1C**). Next, we focus on how Mediator kinase inhibition influenced transcriptional, metabolic, and cytokine responses in IFNγ-treated D21 and T21 cells.

Transcription: The regulatory roles of the Mediator kinases CDK8 and CDK19 are context- and cell type-specific, and their functions appear to be especially important for initiating changes in gene expression programs, such as during an acute stimulus (24). As shown in **Figure 3A**, many of the genes responsive to IFNγ (activated or repressed) were impacted in the opposite way in CA + IFNγ-treated D21 or T21 cells (see also **Fig S5A, B**). This CA-dependent antagonism of IFNγ-response genes is best illustrated with difference heatmaps that compared levels of IFN-dependent transcriptional changes with IFN +CA conditions (i.e. IFN vs. Ctrl – IFN+CA vs. Ctrl; **Fig S5C, D**). An example at the CXCL9 gene is shown in **Figure 3B**; CXCL9 is a pro-inflammatory cytokine. GSEA results also reflected CA-dependent suppression of the transcriptional response to IFNγ. In both D21 and T21 cell lines, IFNγ response and other inflammatory pathways were down-regulated with CA treatment compared with IFNγ alone (**Fig 3C, D; Table S4**). Similar results were obtained with an assessment of inflammatory pathways using IPA (**Fig S5E; Table S5**). For example, pro-inflammatory factors were almost uniformly down-regulated in IFNγ-stimulated, CA-treated cells. Thus, Mediator kinase inhibition blocked normal transcriptional responses to IFNγ, consistent with prior studies in mouse and human cancer cells (12, 14). The up-regulated Hallmark pathways included cholesterol homeostasis and fatty acid metabolism (**Fig 3C, D; Table S4**). A set of factors from the IPA upstream regulators analysis underscores this result, identifying TFs and enzymes involved in cholesterol and lipid metabolism in CA-treated cells T21 cells (**Fig 3E-G**), with similar results in D21 (**Fig S5F, G; Table S5**). These IPA results were consistent with CA-treated cells under basal conditions (**Fig 2B, Fig S3C-F**) and were further supported by metabolomics data from IFN-treated cells (see below).

To probe further, and to correlate our results with data from large-scale cohort studies, we compared the GSEA "leading edge" IFN response gene set from a whole blood transcriptome dataset generated by the Human Trisome Project (11) with the CA-responsive genes in our T21 cell line. As shown in **Figure S5H**, 86% of these genes (69 out of 80) overlapped with those identified as elevated in the Human Trisome Project dataset, reflecting a common transcriptional response to IFNγ. Among these IFN-responsive genes were many whose expression decreased upon CA treatment, including STAT1, IRF1, GBP4, MX2, XCL1, and CXCL9. These results reveal that Mediator kinase inhibition suppresses transcriptional responses that are typically hyperactivated in DS individuals.

DNA-binding TFs are common targets for Mediator kinases (22) and TF phosphorylation contributes to CDK8 and/or CDK19-dependent effects on gene expression (12, 14). To test the notion that Mediator kinases suppress transcriptional responses to IFNγ through TFs, we completed upstream regulators pathway analyses (IPA) based on the RNA-seq data. As shown in **Figure 3F, G** and **Figure S5F, G**, an array of pro-inflammatory TFs were induced in IFNγ-treated T21 and D21 cells, as expected. Strikingly, however, the IFNγ-dependent activation of these same TFs was blocked in CA-treated cells (D21 and T21). These results suggest that inhibition of Mediator kinases suppresses IFNγ responses, in part, through inhibition of pro-inflammatory TF activity, in agreement with prior experiments in CA-treated mouse and human cells (12).

Metabolism: Consistent with the RNA-seq results, metabolic changes in D21 and T21 cells reflected a CA-dependent suppression of IFNγ-induced inflammation. In short, CA treatment reversed metabolic changes induced by IFNγ alone. For example, LCFAs, endocannabinoids,

7

oleamide, desmosterol, and bile acids were reduced in D21 cells under IFNγ-stimulation conditions, consistent with the anti-inflammatory roles of these metabolites (44-48). By contrast, their levels were elevated in CA-treated D21 cells whereas the effects of Mediator kinase inhibition were reduced in scope in IFNγ-treated T21 cells, which may reflect the elevated basal IFN signaling in T21 cells (**Fig 4A–C; Table S9**). As in D21 cells, however, the CA-dependent changes in T21 were generally the opposite of those caused by IFNγ treatment alone, consistent with an anti-inflammatory effect (**Fig 4B, C; Table S9**). For instance, quinolinic acid, a tryptophan derivative that is elevated in DS (40), was elevated in T21 cells following IFNγ stimulation but this was blocked by CA treatment (**Fig 4C**; **Table S9**). Collectively, the data summarized in **Figure 4A–C** and **Table S9** reveal that CA-dependent changes in immunomodulatory lipids were opposite those induced by IFNγ treatment alone, consistent with CA-dependent anti-inflammatory effects.

Cytokines: Compared with basal conditions, many more cytokines showed CA-responsiveness in the context of IFNγ stimulation, and a majority of the changes countered IFNγ-induced inflammatory responses (**Fig S6A**). This CA-dependent antagonism of IFNγ cytokine responses is perhaps best illustrated in the difference heatmaps shown in **Figure 4D, E**, which show the widespread suppressive effect of CA treatment on IFNγ-induced cytokine levels. Levels of many pro-inflammatory cytokines were reduced in IFNγ + CA-treated D21 and T21 cells, including CXCL9, C5, IL33, IL1α, and others (**Fig S6A**).

Because cytokine levels were measured 24h after treatment, we hypothesized that their altered levels would at least partially correspond to gene expression changes that were measured earlier, at 4h post-treatment. Indeed, this was observed for many IFNγ-induced cytokines impacted by Mediator kinase inhibition, as shown in **Figure S6B**. (Note that expression changes for cytokine receptors are also shown.) For example, gene expression changes for CXCL9, CXCL10, MIP1α/β (a.k.a. CCL3/4), FLT3 ligand, GCSF, MCSF, IL10, IL24, and TFR tracked with changes in their cytokine levels in CA-treated cells (**Fig S6B**; compare with **Fig 2F**). Collectively, the cytokine screen results demonstrated that inhibition of Mediator kinase function generally antagonized IFNγ signaling by downregulating pro-inflammatory cytokines while upregulating anti-inflammatory cytokines (e.g IL10, LIF, IL19). In the context of Down syndrome, this could potentially mitigate pathological immune system hyperactivation.

Mediator kinases regulate splicing in pathway- and cell type-specific ways

As Mediator-associated kinases, CDK8 and CDK19 are established regulators of RNAPII transcription (24); however, their potential impact on splicing has not been examined. Over 95% of human mRNAs are alternatively spliced and defects in this process are major contributors to errors in gene expression in human diseases (52). Because we sequenced total mRNA at a depth of ≥ 115 million mapped reads/replicate, we were poised to examine whether Mediator kinase inhibition affected RNAPII splicing.

We completed analysis of alternative splicing events using rMATS (53), separately evaluating all RNA-seq replicates (biological triplicates; **Fig 1A**). The data revealed 741 differential exon skipping events in T21 cells (vs. D21) under basal conditions (**Fig 5A, B**; **Table S10**), with approximately equal numbers of alternative exon inclusion events (n=382) compared with alternative exon skipping events (n=359). By contrast, other alternative splicing events (e.g. intron retention) were less affected (**Fig S7A**). We observed similar trends in IFNγ-treated T21 and D21 cells, in which a greater number of exon skipping events (n=418 vs. n=296) occurred in IFNγ-stimulated T21 cells vs. D21 cells, whereas other alternative splicing events were less common (**Fig S7B, C; Table S10**).

To determine whether Mediator kinase activity might regulate splicing, we next evaluated CA-treated D21 and T21 cells. We found that CA treatment had a substantial impact on splicing,

in both D21 and T21 cells (**Fig 5C** & **Fig S7D**). We identified 432 or 444 sites with altered exon skipping events (D21 or T21, respectively) in CA-treated cells compared with controls (ΔPSI [percent spliced in]≥ 0.2, Padj < 0.05; **Fig 5C, Table S10**), and CA treatment increased inclusion of alternative exons more frequently than it increased their skipping in both lines (n=239 vs. 193 in D21; n=256 vs. 188 in T21). Additional evidence for Mediator kinase-dependent regulation of splicing derived from analysis of CA-dependent effects in IFNγ-treated D21 and T21 cells (**Fig 5D, E; Table S10**). Here as well, Mediator kinase inhibition primarily impacted exon skipping events (compared with other potential splicing changes; **Fig S7E**), with hundreds of sites showing increased inclusion (n=178 in D21; 213 in T21) or increased skipping (n=130 in D21; 148 in T21) of alternative exons.

To assess whether the exon skipping events selectively affected specific gene sets, we completed pathway analyses (IPA) across all conditions tested (**Fig 5F-H; Fig S7F, G; Table S5**). To increase statistical power, we grouped exon skipping events together (i.e. alternative exon inclusion events + alternative exon skipping events). Thus, the T21 vs. D21 comparison included 741 events (affecting a maximum of 741 genes), D21 +CA vs. Ctrl included 432 events, and so on. The results revealed that splicing changes triggered by Mediator kinase inhibition were cell type specific (T21 vs. D21) and selectively impacted inflammatory and metabolic pathway genes. As shown in **Figure 5F**, genes associated with inflammatory signaling (red highlighted pathways) were differentially spliced in CA-treated T21 cells (vs. D21) during IFNγ stimulation. In addition, pyrimidine salvage and biosynthesis genes were alternatively spliced in CA-treated T21 cells (**Fig 5H**). These pathway-specific effects in CA-treated cells were consistent with pathway-specific changes in gene expression (e.g. GSEA Hallmark gene sets, **Table S4**) and with metabolic changes observed in CA-treated cells. For instance, the pyrimidine biosynthesis intermediates N-carbamoylaspartate, dihydroorotate, and orotate were markedly depleted in CA-treated T21 cells but not control cells (**Table S2**). The data in **Figure 5H** implicate CA-dependent splicing changes as a contributing factor.

Collectively, the data summarized in **Figure 5** and **Figure S7** establish the Mediator kinases CDK8 and CDK19 as regulators of splicing, thus identifying a novel means by which these kinases govern RNAPII gene expression. The data also identify kinase-dependent splicing regulation as an additional mechanism by which CDK8 and/or CDK19 act in stimulus-specific (i.e. IFNγ) and cell type-specific ways (i.e. T21 vs. D21).

Discussion

Previous studies have shown that Mediator kinases regulate transcriptional responses to inflammatory stimuli (e.g. IFNγ or TNFα) in a variety of model systems (12, 15). Because individuals with Down syndrome have chronic, hyperactive IFN signaling (6), we hypothesized that Mediator kinase inhibition would antagonize inflammatory signaling cascades in T21 cells. This hypothesis was supported by the experimental results described here, which showed that Mediator kinase inhibition antagonizes inflammatory pathways at the transcriptional, metabolic, and cytokine protein levels. Collectively, our results have expanded upon established concepts for CDK8 and CDK19 (e.g. regulation of IFNγ signaling) by revealing new insights about their impact on metabolic and cytokine responses, as well as their function in pre-mRNA splicing; furthermore, our results establish Mediator kinases as potential therapeutic targets to antagonize hyperactive IFN signaling in DS.

We acknowledge that individual-to-individual genetic variation could contribute to the differences we observe in our T21 vs. D21 comparisons (6, 34). We chose cell lines from sibling donors (both males of similar age) to minimize this possibility. Moreover, cross-referencing our results with data collected from large cohorts of individuals of varying age and sex (with/without

T21) showed broadly similar trends in transcript (11), metabolite (40), and cytokine levels (32) in the T21/D21 comparisons. Although our multi-omics T21/D21 comparisons yielded new insights, we emphasize that Mediator kinases were a focus of this study, and the T21/D21 comparisons served as benchmarks to assess CDK8/CDK19 function in the physiologically relevant contexts of DS and IFNγ signaling. A limitation of this study is that additional donor-derived cell lines were not evaluated; furthermore, the transcriptomic, metabolomic, and cytokine data were collected at one time point, such that temporal trends in IFNγ responses can only be inferred (see below).

CDK8 and CDK19 kinase activity impacts core metabolic pathways
Metabolomics has been described as the most direct readout of cell state, yielding a "front line" assessment through quantitation of the biochemicals that drive all cellular processes (25). The role of Mediator kinases in human cell metabolism is poorly understood. As a whole, our metabolomics data revealed the most striking CDK8/CDK19 effects on nucleotide biosynthesis and lipid homeostasis. Nucleotide levels (purines and pyrimidines) and their intermediates were broadly reduced in CA-treated cells whereas different classes of lipids were generally elevated (**Table S8**).

The gene expression changes (RNA-seq, 4h) triggered by Mediator kinase inhibition tracked with these "downstream" metabolic changes (24h), suggesting that Mediator kinases primarily affect metabolism indirectly (e.g. **Fig 2B, Fig S3E**). For example, nucleotide biosynthesis genes were down-regulated whereas lipid metabolism genes were up-regulated in CA-treated cells; this was reflected in the GSEA Hallmarks, with positive enrichment for pathways such as cholesterol homeostasis, bile acid metabolism, and FA metabolism and negative enrichment for DNA repair pathways, which contains many nucleotide biosynthesis genes. Pyrimidine metabolism genes were also alternatively spliced in CA-treated cells (see below). The differential timing of the transcriptomics and metabolomics experiments helps link metabolic changes to gene expression changes; however, CA-induced gene expression changes will only partially account for altered metabolite levels and we cannot exclude other factors and pathways. For example, reduced levels of nucleotides can trigger cellular compensation through up-regulation of FA levels (54). Consequently, elevated levels of FA and other lipids may result, in part, from compensatory mechanisms triggered by CA-dependent reductions in nucleotide levels.

Pathway-specific regulation of splicing by Mediator kinases
Despite widespread study of Mediator kinases as regulators of RNAPII transcription, their potential function in splicing has not been addressed. We hypothesized that CDK8 and/or CDK19 may impact splicing based upon prior results that identified NAB2, SRRM2, and KDM3A as high-confidence CDK8/CDK19 substrates in human cells (22); each of these proteins has been linked to regulation of splicing (55-57). Our analysis revealed that exon skipping was dependent upon the kinase function of CDK8 and/or CDK19; increased inclusion of alternative exons was observed at hundreds of sites whereas increased skipping occurred at hundreds of additional sites in CA-treated cells (D21 or T21), and this was observed under both basal and IFNγ-stimulated conditions (**Fig 5C, D**).

Pathway analysis of the alternatively spliced genes in CA-treated cells identified gene sets associated with signaling pathways known to be regulated by Mediator kinases, such as TGFβ and interferon signaling (**Fig 5F**). Interestingly, CA-dependent alternative splicing of these gene sets occurred specifically in IFNγ-stimulated T21 cells (not D21); moreover, other pathways were selectively affected by Mediator kinase inhibition in cell type and context-specific ways. For instance, mTOR pathway genes in CA-treated D21 cells and pyrimidine metabolism genes in T21 cells (**Fig 5G, H**).

Taken together, these results establish the Mediator kinases as regulators of RNAPII splicing, which adds to the mechanisms by which CDK8 and CDK19 can influence RNAPII transcription. Our data reveal that kinase-dependent splicing regulation occurs in cell type- and context-specific ways, similar to other known regulatory functions for CDK8 and CDK19 (24). We have also shown that CDK8/CDK19-dependent splicing regulation contributes to kinase-dependent biological outcomes; for example, genes that control pyrimidine biosynthesis and salvage pathways were selectively impacted by alternative splicing in CA-treated T21 cells, and these cells had markedly reduced levels (1.4 – 3 fold) of pyrimidine intermediates N-carbamoylaspartate, dihydro-orotate, and orotate compared with untreated T21 controls (**Table S8**). The precise mechanisms by which CDK8 and/or CDK19 impact these splicing events remain unclear, but are likely to involve both direct kinase-dependent regulation of splicing factors (e.g. through phosphorylation of NAB2 or SRRM2) and indirect regulation through modification of DNA-binding TFs (58), which are common Mediator kinase substrates (22). Differential expression of splicing regulatory proteins in CA-treated cells may also contribute, although the time frames of our analyses (RNA-seq at 4h post-treatment) minimize this possibility.

Mediator kinase inhibition broadly antagonizes IFN signaling

Independently and collectively, our transcriptomics, metabolomics, and cytokine screen data revealed that Mediator kinase inhibition suppressed pro-inflammatory signaling. This was most evident during IFNγ stimulation but was also apparent under basal conditions, especially in T21 cells due to their high "baseline" activation of IFN signaling pathways. We acknowledge that metabolites and cytokines can have variable, dynamic, and context-specific effects on inflammatory signaling. For example, sphingolipids (59) and bile acids may serve pro- or anti-inflammatory roles depending upon cell type (60), and cytokine responses are complex, in part because cytokines regulate each other (e.g. MIP3α/CCL20 is down-regulated by IL10). For this study, an alternative and more straightforward metric for an anti-inflammatory change is whether CA treatment countered the effect of IFNγ stimulation alone. This was observed in an overwhelming number of cases across all experiments (RNA-seq, metabolomics, cytokine screen).

Among the IFNγ-responsive genes (i.e. up- or down-regulated in response to IFNγ), the expression of many shifted in the opposite direction in IFNγ +CA conditions (**Fig 3A**). Based upon the RNA-seq data, IPA predicted CA-dependent inhibition of IFN-responsive TFs such as IRF1, IRF5, IRF7, NFKB1, and STAT1 (**Fig 3F, G; Fig S5F, G**). Consistent with these findings, prior results from our labs have shown that IFN-responsive TFs fail to activate when CDK8 and CDK19 are inhibited (12), and DNA-binding TFs, including STAT1 (14), represent high-confidence Mediator kinase substrates (22). Comparison of our T21 transcriptomics data with an RNA-seq analysis of whole blood from a large cohort of DS individuals (11) identified a similar set of IFNγ-induced genes (**Fig S5H**), linking our results to the general population. Importantly, expression of most of these so-called IFN "leading edge" genes was reduced upon Mediator kinase inhibition in T21 cells, suggesting that Mediator kinases help drive pro-inflammatory signaling in DS individuals.

To our knowledge, there has been no large-scale analysis of Mediator kinase-dependent effects on cytokine responses, despite much evidence that CDK8 and/or CDK19 help control inflammatory responses in a variety of mammalian cell types (12, 15, 16, 19). Our screen of over 100 cytokines revealed that Mediator kinases control cytokine signaling under basal and IFNγ-stimulated conditions and generally had a pro-inflammatory effect (i.e. CDK8/CDK19 inhibition was anti-inflammatory). As with the transcriptional and metabolic changes, Mediator kinase inhibition reversed many IFNγ-induced changes in cytokine levels (**Fig 4D, E**). DS was recently characterized as a "cytokinopathy" and basal levels of as many as 22 cytokines were identified (among a screen of 29 cytokines) as highly elevated in the plasma of DS individuals (32). At least

6 of these 22 cytokines were reduced upon CA treatment in T21 cells (GMCSF, IL1α, IL3, IL13, IL15, GCSF), again suggesting that Mediator kinases drive inflammatory signaling in DS.

The CA-dependent metabolic changes also consistently reversed IFNγ-dependent effects; however, IFNγ treatment caused metabolic changes that were distinct in D21 vs. T21 cells. Interestingly, Mediator kinase inhibition increased levels of anti-inflammatory lipid signaling molecules (e.g. endocannabinoids, desmosterol, LCFA) in T21 cells under basal conditions (**Fig 2C**), whereas similar changes were observed in IFNγ stimulated D21 cells (**Fig 4A**). We hypothesize that this results from the elevated basal IFN signaling in T21 cells, such that CA treatment could measurably suppress chronic, active inflammatory pathways in the absence of exogenous IFNγ stimulation. The ability of CA to antagonize the "basal" inflammatory signaling in T21 cells suggests a potential therapeutic strategy to mitigate the chronic immune system dysregulation in individuals with DS (36).

The anti-inflammatory lipids that were elevated in CA-treated cells included oleamide, desmosterol, endocannabinoids such as oleoylethanolamide, and PUFAs such as EPA, DPA, DHA and various other ω3 or ω6 PUFAs. These metabolites act as signaling molecules, at least in part, through binding nuclear receptors or GPCRs such as FFAR1, FFAR4, and GPR119, to initiate a cascade of anti-inflammatory responses (44-47, 49). The wide-ranging impact of Mediator kinase inhibition on these lipid mediators of inflammation reveals new mechanisms by which CDK8 and/or CDK19 help control cellular responses to IFNγ; these results also raise new questions about how Mediator kinases influence basic biological processes (**Fig 6**). Future projects could more directly probe TF responses in CA-treated cells or track transcriptome and/or metabolome changes at greater temporal resolution.

Working model: CDK8/19 inhibition enables persistent suppression of IFN signaling
Given the well-established roles for CDK8 and CDK19 as regulators of RNAPII transcription (24), the majority of direct CA-dependent effects likely result from gene expression changes. This hypothesis is also consistent with phosphoproteomics data that identified TFs and other RNAPII regulatory factors as high-confidence targets of CDK8/CDK19 in human cells (22). The staggered timing of our RNA-seq (4 hr), metabolomics (24 hr), and cytokine screen experiments (24 hr) allow inference of direct vs. indirect effects of Mediator kinase inhibition. Taken as a whole, our results suggest that CDK8/CDK19 inhibition initiates a cascade of events that reinforce and propagate anti-inflammatory responses over time (**Fig 6**). Transcriptomics data identified SREBP (IPA upstream regulators), cholesterol homeostasis and fatty acid metabolism (GSEA Hallmarks) as activated upon Mediator kinase inhibition. Notably, SREBP TFs activate cholesterol and fatty acid biosynthesis pathways. Metabolomics data revealed elevated levels of an array of anti-inflammatory lipids in CA-treated cells during IFNγ signaling (e.g. D21 cells +IFNγ; T21 cells at basal conditions). Among these elevated lipids, oleamide, desmosterol, and PUFAs are nuclear receptor agonists that activate PPAR and LXR (61-64); PPAR and LXR, in turn, broadly control fatty acid biosynthesis (65), including PUFAs such as DPA, DHA, and EPA, whose levels were consistently elevated in CA-treated cells. These and other PUFAs bind GPCRs such as FFAR1/4 (45) to drive anti-inflammatory signaling cascades in an autocrine or paracrine manner. In this way, Mediator kinase inhibition may robustly and durably antagonize IFN signaling via metabolites that act downstream of initial gene expression changes (**Fig 6**).

Concluding remarks
Although the factors that contribute to the DS condition are complex (3), it has been described as both an interferonopathy (6) and a cytokinopathy (32). Accordingly, an emerging theme in DS research is that individuals with DS could benefit from therapeutic strategies that diminish chronic,

hyperactive IFN signaling (11, 36, 66). At least one clinical trial with a JAK inhibitor is underway (NCT04246372). A mouse model of DS showed that multiple phenotypes associated with this condition were driven by triplication of the INFR gene cluster, including cognitive and developmental delays and heart defects (11). These and other studies implicate hyperactive IFN signaling as central to the DS condition (32, 36). Through multi-omics evaluation of CA-dependent effects in T21 cells, we have demonstrated that Mediator kinase inhibition robustly and durably antagonizes hyperactive IFN signaling, via diverse mechanisms that extend beyond transcription (**Fig 6**). Consequently, selective inhibition of Mediator kinase function represents a potential therapeutic strategy to address chronic inflammation and its associated co-morbidities in DS.

Materials & Methods

Cell culture

Immortalized lymphoblastoid cell lines derived from age- and sex-matched sibling pairs (one D21: TIC0002294, one T21: TIC0001678) were obtained from the Nexus Biobank. Cells were cultured in RPMI medium (Gibco, 23400062) supplemented with 20% fetal bovine serum (Peak Serum Inc, PS-FB3), 1x GlutaminePlus (R&D Systems, R90210), and 1x Penicillin-Streptomycin (Gibco, 15140-163), on low-attachment flasks at 37C and 5% CO_2. Due to the lower proliferation rate of T21 cells compared to D21 cells, T21 cells were seeded at twice the density of D21 cells for all experiments unless otherwise noted.

RT-qPCR

Cells were seeded and allowed to recover for 24 hours prior to being treated with 10 ng/mL interferon gamma (Gibco PHC4031) or vehicle (40 mM Tris pH 7.4). Total RNA was isolated using TRizol (Invitrogen, 15596026) according to the manufacturer's instructions, quantified with a Qubit® 3.0 using the RNA High Sensitivity (HS) kit (Invitrogen™, Q32855), and 100 ng of RNA from each sample was converted to cDNA using High-Capacity cDNA Reverse Transcription Kit (Applied Biosystems, 4368813) following the manufacturer's instructions. cDNA was diluted to 0.25 ng/μL for all samples, and amplification was performed using Sybr Select Master Mix (Thermo Fisher Scientific, 4472908) on a BioRad CFX384 Real Time PCR System. ΔΔCT values were calculated using GAPDH as a load control. Treatments, RNA isolation, and RT-qPCR were performed in biological duplicate. The primers used for qPCR are as follows - GAPDH Forward: ACCACAGTCCATGCCATCAC, GAPDH Reverse: TCCACCACCCTGTTGCTGTA, GBP1 Forward: GTGCTAGAAGCCAGTGCTCGT, GBP1 Reverse: TGGGCCTGTCATGTGGATCTC, IRF1 Forward: GAGGAGGTGAAAGACCAGAGC, IRF1 Reverse: TAGCATCTCGGCTGGACTTCGA.

To probe the timing of the RNA-seq experiments, we completed RT-qPCR at various time points as shown in **Figure S1A**. The 4h time point (post-IFNγ) was chosen because robust induction of GBP1 and IRF1 mRNA was observed. Whereas mRNA levels remained high at 6h, we selected the 4h time point because it would better represent the primary transcriptional response; moreover, the 4h time point was consistent with prior transcriptomics studies of IFNγ response in mammalian cells (12).

Metabolomics

For each treatment condition, six flasks of cells were seeded and allowed to recover for 24 hours prior to treatment. Cells were pre-treated with 0.1% DMSO or 100 nM cortistatin A for one hour, then treated with 40 mM Tris, pH 7.4 or 10 ng/mL interferon gamma (Gibco, PHC4031). After 24 hours of interferon gamma treatment, cells were harvested and snap-frozen in liquid nitrogen. Sample preparation was carried out by Metabolon (Durham, North Carolina, USA) using a previously published workflow (67). Samples were prepared using the automated MicroLab STAR® system from Hamilton Company, and several recovery standards were added prior to the first step in the extraction process for QC purposes. To remove protein, dissociate small molecules bound to protein or trapped in the precipitated protein matrix, and to recover chemically diverse metabolites, proteins were precipitated with methanol under vigorous shaking for 2 min (Glen Mills GenoGrinder 2000) followed by centrifugation. The resulting extract was divided into five fractions: two for analysis by two separate reverse phase (RP)/UPLC-MS/MS methods with positive ion mode electrospray ionization (ESI), one for analysis by RP/UPLC-MS/MS with negative ion mode ESI, one

for analysis by HILIC/UPLC-MS/MS with negative ion mode ESI, and one sample was reserved for backup. Samples were placed briefly on a TurboVap® (Zymark) to remove the organic solvent.

All methods utilized a Waters ACQUITY ultra-performance liquid chromatography (UPLC) and a Thermo Scientific Q-Exactive high resolution/accurate mass spectrometer interfaced with a heated electrospray ionization (HESI-II) source and Orbitrap mass analyzer operated at 35,000 mass resolution. The sample extract was dried then reconstituted in solvents compatible to each of the four methods. Each reconstitution solvent contained a series of standards at fixed concentrations to ensure injection and chromatographic consistency. One aliquot was analyzed using acidic positive ion conditions, chromatographically optimized for more hydrophilic compounds. In this method, the extract was gradient eluted from a C18 column (Waters UPLC BEH C18-2.1x100 mm, 1.7 μm) using water and methanol, containing 0.05% perfluoropentanoic acid (PFPA) and 0.1% formic acid (FA). Another aliquot was also analyzed using acidic positive ion conditions, however it was chromatographically optimized for more hydrophobic compounds. In this method, the extract was gradient eluted from the same afore mentioned C18 column using methanol, acetonitrile, water, 0.05% PFPA and 0.01% FA and was operated at an overall higher organic content. Another aliquot was analyzed using basic negative ion optimized conditions using a separate dedicated C18 column. The basic extracts were gradient eluted from the column using methanol and water, however with 6.5mM Ammonium Bicarbonate at pH 8. The fourth aliquot was analyzed via negative ionization following elution from a HILIC column (Waters UPLC BEH Amide 2.1x150 mm, 1.7 μm) using a gradient consisting of water and acetonitrile with 10mM Ammonium Formate, pH 10.8. The MS analysis alternated between MS and data-dependent MSn scans using dynamic exclusion. The scan range varied slighted between methods but covered 70-1000 m/z.

Identification of metabolites was performed through automated comparison of the ion features in experimental samples to a reference library of chemical standard entries (68), and are based on three criteria: retention index within a narrow RI window of the proposed identification, accurate mass match to the library +/- 10 ppm, and the MS/MS forward and reverse scores between the experimental data and authentic standards. The MS/MS scores are based on a comparison of the ions present in the experimental spectrum to the ions present in the library spectrum. While there may be similarities between these molecules based on one of these factors, the use of all three data points can be utilized to distinguish and differentiate biochemicals.

Statistical and pathway analysis of metabolomics data
Two types of statistical analyses were performed: (1) significance tests and (2) classification analysis. Standard statistical analyses were performed in Array Studio on log-transformed data. For analyses not standard in Array Studio, the R program (http://cran.r-project.org/) was used. Following log transformation and imputation of missing values, if any, with the minimum observed value for each compound, Welch 2-sample *t* test was used as a significance test to identify biochemicals that differed significantly ($p < 0.05$) between experimental groups. An estimate of the false discovery rate (q-value) was calculated to take into account the multiple comparisons that normally occur in metabolomic-based studies. Classification analyses included principal component analysis (PCA), hierarchical clustering, and random forest.

Pathway analysis of metabolomic data was performed using the Ingenuity Pathway Analysis software (Qiagen) (37). For metabolomic analysis, a total of 566 out of 675 metabolites could be mapped using one of the following identifiers: CAS registry number, Human Metabolome Database (HMDB) identification, KEGG, PubChem CID, or RefSeq number; metabolites not used in IPA analysis can be found in **Table S2**. Metabolomic pathway analysis used only mapped metabolites with a p-value of <0.1 when making pathway predictions.

RNA-seq
Cells were pre-treated with 0.1% DMSO or 100 nM cortistatin A for 30 minutes, then treated with 40 mM Tris, pH 7.4 or 10 ng/mL interferon gamma (Gibco, PHC4031). After four hours, total RNA was isolated from D21 or T21 cells using TRizol (Invitrogen, 15596026) as specified by the manufacturer and quantified with a Qubit® 3.0 using the RNA High Sensitivity (HS) kit (Invitrogen™, Q32855). 1 µg of total RNA with a RIN number of ≥8 was used for RNA-seq library prep. Libraries were constructed using Universal Plus™ mRNA-

Seq library preparation kit with NuQuant® (Tecan, 0520). Library construction and sequencing were performed at the Genomics Shared Resource (CU Anschutz). Paired-end libraries (151 bp x 151 bp) were sequenced on the Illumina NextSeq 6000 platform (Firmware version 1.26.1, RTA version: v3.4.4, Instrument ID: A00405).

RNA-seq sequencing and computational analysis

For differential gene expression analysis, the workflow was as follows: adaptor sequences were trimmed from the RNA-seq raw fastq files using BBDuk (https://sourceforge.net/projects/bbmap/) and mapped using HISAT2(69). Gene counts were generated using featureCounts(70), and differential expression analysis was performed using DESeq2 (71). Duplicate genes were filtered and those with the highest FPKM were kept for analysis. For inter-genotype (T21 vs D21) comparisons, expression of genes on chromosome 21 was normalized to ploidy. While ERCC RNA Spike-In Mix (Invitrogen™, 4456740) was added to isolated RNA samples prior to sequencing, ERCC gene counts were variable across vehicle treated samples even after accounting for read depth, and when using multiple normalization methods and a linear regression. As such, the median of ratios method native to DESeq2 was used to generate size factors and normalize samples. Qiagen ingenuity pathway analysis (IPA) version 90348151 (37), GSEA 4.2.3 (35), and Gene Ontology analysis (72) were used for identification of activated and inhibited pathways. For IPA analysis, a total of 27,647 out of 28,265 genes could be mapped using Entrez Gene Symbols. For cross-genotype (i.e. T21 vs D21) pathway analysis, only genes with a fold-change > |1.25| and adjusted p-value <0.1 were used. For within-genotype (i.e. treatment effects) pathway analysis, only genes with an adjusted p-value <0.1 were used.

For splicing analysis, the workflow was as follows: duplicates were removed and adaptors trimmed using the bbTools function (v39.01), trimmed reads were mapped uniquely against the hg38 genome using HISAT2 (v2.1.0) (69), mapped reads were processed with rMATS (v4.0.1) (53), and results were filtered based on FDR < 0.05, absolute(IncLevelDifference) < 0.2, and ≥2 reads/replicate. Sashimi plots were generated from rMATS results using a modified script based on ggsashimi.py.

The data in this publication have been deposited in NCBI's Gene Expression Omnibus and are accessible through GEO Series accession number GSE220652. The code used to process and visualize the data can be found at https://github.com/kira-alia/Cozzolino2023.

Cytokine screen

Cells were pre-treated with 0.1% DMSO or 100 nM cortistatin A for 30 minutes, then treated with 40 mM Tris, pH 7.4 or 10 ng/mL interferon gamma (Gibco, PHC4031). After 24 hours, cells were lysed in RIPA buffer (Thermo Scientific, 89900) supplemented with Halt™ Protease and Phosphatase Inhibitor Cocktail, EDTA-free (100X) (Thermo Scientific, 78441) and Benzonase® endonuclease (Millipore Sigma, 101697). Lysate concentrations were determined using the Pierce™ BCA Protein Assay Kit (Thermo Scientific, 23225), and 250 µg of protein from each condition was incubated with a membrane array from the Proteome Profiler Human XL Cytokine Array Kit (R&D Systems, ARY022B). Membranes were processed according to the manufacturer's instructions and imaged using an ImageQuant LAS 4000 (GE Healthcare). Background-subtracted technical replicate values for each cytokine in each condition were quantified using ImageJ and averaged giving a normalized intensity value. The relative intensity was compared on a per cytokine basis and was statistically assessed using a one-way ANOVA test between the eight total conditions across two biological replicates.

Acknowledgments

References

1. G. de Graaf, F. Buckley, B. G. Skotko, Estimation of the number of people with Down syndrome in the United States. *Genet Med* **19**, 439-447 (2017).

2. S. E. Antonarakis, Down syndrome and the complexity of genome dosage imbalance. *Nature reviews. Genetics* **18**, 147-163 (2017).

3. S. E. Antonarakis, B. G. Skotko, M. S. Rafii, A. Strydom, S. E. Pape, D. W. Bianchi, S. L. Sherman, R. H. Reeves, Down syndrome. *Nat Rev Dis Primers* **6**, 9 (2020).

4. H. Hasle, I. H. Clemmensen, M. Mikkelsen, Risks of leukaemia and solid tumours in individuals with Down's syndrome. *Lancet* **355**, 165-169 (2000).

5. P. Araya, K. A. Waugh, K. D. Sullivan, N. G. Nunez, E. Roselli, K. P. Smith, R. E. Granrath, A. L. Rachubinski, B. Enriquez Estrada, E. T. Butcher, R. Minter, K. D. Tuttle, T. C. Bruno, M. Maccioni, J. M. Espinosa, Trisomy 21 dysregulates T cell lineages toward an autoimmunity-prone state associated with interferon hyperactivity. *Proc Natl Acad Sci U S A* **116**, 24231-24241 (2019).

6. K. D. Sullivan, H. C. Lewis, A. A. Hill, A. Pandey, L. P. Jackson, J. M. Cabral, K. P. Smith, L. A. Liggett, E. B. Gomez, M. D. Galbraith, J. DeGregori, J. M. Espinosa, Trisomy 21 consistently activates the interferon response. *eLife* **5**, e16220 (2016).

7. K. A. Waugh, P. Araya, A. Pandey, K. R. Jordan, K. P. Smith, R. E. Granrath, S. Khanal, E. T. Butcher, B. E. Estrada, A. L. Rachubinski, J. A. McWilliams, R. Minter, T. Dimasi, K. L. Colvin, D. Baturin, A. T. Pham, M. D. Galbraith, K. W. Bartsch, M. E. Yeager, C. C. Porter, K. D. Sullivan, E. W. Hsieh, J. M. Espinosa, Mass Cytometry Reveals Global Immune Remodeling with Multi-lineage Hypersensitivity to Type I Interferon in Down Syndrome. *Cell reports* **29**, 1893-1908 e1894 (2019).

8. D. Bush, C. Galambos, D. Dunbar Ivy, Pulmonary hypertension in children with Down syndrome. *Pediatr Pulmonol* 10.1002/ppul.24687 (2020).

9. V. Madan, J. Williams, J. T. Lear, Dermatological manifestations of Down's syndrome. *Clin Exp Dermatol* **31**, 623-629 (2006).

10. K. Marild, O. Stephansson, L. Grahnquist, S. Cnattingius, G. Soderman, J. F. Ludvigsson, Down syndrome is associated with elevated risk of celiac disease: a nationwide case-control study. *J Pediatr* **163**, 237-242 (2013).

11. K. A. Waugh, R. Minter, J. Baxter, C. Chi, M. D. Galbraith, K. D. Tuttle, N. P. Eduthan, K. T. Kinning, Z. Andrysik, P. Araya, H. Dougherty, L. N. Dunn, M. Ludwig, K. A. Schade, D. Tracy, K. P. Smith, R. E. Granrath, N. Busquet, S. Khanal, R. D. Anderson, L. L. Cox, B. E. Estrada, A. L. Rachubinski, H. R. Lyford, E. C. Britton, K. A. Fantauzzo, D. J. Orlicky, J. L. Matsuda, K. Song, T. C. Cox, K. D. Sullivan, J. M. Espinosa, Triplication of the interferon receptor locus contributes to hallmarks of Down syndrome in a mouse model. *Nature genetics* **55**, 1034-1047 (2023).

12. I. Steinparzer, V. Sedlyarov, J. D. Rubin, K. Eislmayr, M. D. Galbraith, C. B. Levandowski, T. Vcelkova, L. Sneezum, F. Wascher, F. Amman, R. Kleinova, H. Bender, Z. Andrysik, J. M. Espinosa, G. Superti-Furga, R. D. Dowell, D. J. Taatjes, P. Kovarik, Transcriptional

Responses to IFN-gamma Require Mediator Kinase-Dependent Pause Release and Mechanistically Distinct CDK8 and CDK19 Functions. *Mol Cell* **76**, 485-499 (2019).

13. H. E. Pelish, B. B. Liau, Nitulescu, II, A. Tangpeerachaikul, Z. C. Poss, D. H. Da Silva, B. T. Caruso, A. Arefolov, O. Fadeyi, A. L. Christie, K. Du, D. Banka, E. V. Schneider, A. Jestel, G. Zou, C. Si, C. C. Ebmeier, R. T. Bronson, A. V. Krivtsov, A. G. Myers, N. E. Kohl, A. L. Kung, S. A. Armstrong, M. E. Lemieux, D. J. Taatjes, M. D. Shair, Mediator kinase inhibition further activates super-enhancer-associated genes in AML. *Nature* **526**, 273-276 (2015).

14. J. Bancerek, Z. C. Poss, I. Steinparzer, V. Sedlyarov, T. Pfaffenwimmer, I. Mikulic, L. Dolken, B. Strobl, M. Muller, D. J. Taatjes, P. Kovarik, CDK8 Kinase Phosphorylates Transcription Factor STAT1 to Selectively Regulate the Interferon Response. *Immunity* **38**, 250-262 (2013).

15. M. Chen, J. Liang, H. Ji, Z. Yang, S. Altilia, B. Hu, A. Schronce, M. S. J. McDermott, G. P. Schools, C. U. Lim, D. Oliver, M. S. Shtutman, T. Lu, G. R. Stark, D. C. Porter, E. V. Broude, I. B. Roninson, CDK8/19 Mediator kinases potentiate induction of transcription by NFkappaB. *Proc Natl Acad Sci U S A* **114**, 10208-10213 (2017).

16. K. A. Freitas, J. A. Belk, E. Sotillo, P. J. Quinn, M. C. Ramello, M. Malipatlolla, B. Daniel, K. Sandor, D. Klysz, J. Bjelajac, P. Xu, K. A. Burdsall, V. Tieu, V. T. Duong, M. G. Donovan, E. W. Weber, H. Y. Chang, R. G. Majzner, J. M. Espinosa, A. T. Satpathy, C. L. Mackall, Enhanced T cell effector activity by targeting the Mediator kinase module. *Science* **378**, eabn5647 (2022).

17. Z. Guo, G. Wang, Y. Lv, Y. Y. Wan, J. Zheng, Inhibition of Cdk8/Cdk19 Activity Promotes Treg Cell Differentiation and Suppresses Autoimmune Diseases. *Front Immunol* **10**, 1988 (2019).

18. M. H. Hofmann, R. Mani, H. Engelhardt, M. A. Impagnatiello, S. Carotta, M. Kerenyi, S. Lorenzo-Herrero, J. Bottcher, D. Scharn, H. Arnhof, A. Zoephel, R. Schnitzer, T. Gerstberger, M. P. Sanderson, G. Rajgolikar, S. Goswami, S. Vasu, P. Ettmayer, S. Gonzalez, M. Pearson, D. B. McConnell, N. Kraut, N. Muthusamy, J. Moll, Selective and potent CDK8/19 inhibitors enhance NK cell activity and promote tumor surveillance. *Molecular cancer therapeutics* **19**, 1018-1030 (2020).

19. L. Johannessen, T. B. Sundberg, D. J. O'Connell, R. Kolde, J. Berstler, K. J. Billings, B. Khor, B. Seashore-Ludlow, A. Fassl, C. N. Russell, I. J. Latorre, B. Jiang, D. B. Graham, J. R. Perez, P. Sicinski, A. J. Phillips, S. L. Schreiber, N. S. Gray, A. F. Shamji, R. J. Xavier, Small-molecule studies identify CDK8 as a regulator of IL-10 in myeloid cells. *Nature chemical biology* **13**, 1102-1108 (2017).

20. S. Yamamoto, T. Hagihara, Y. Horiuchi, A. Okui, S. Wani, T. Yoshida, T. Inoue, A. Tanaka, T. Ito, Y. Hirose, Y. Ohkuma, Mediator cyclin-dependent kinases upregulate transcription of inflammatory genes in cooperation with NF-kappaB and C/EBPbeta on stimulation of Toll-like receptor 9. *Genes Cells* **22**, 265-276 (2017).

21. M. Akamatsu, N. Mikami, N. Ohkura, R. Kawakami, Y. Kitagawa, A. Sugimoto, K. Hirota, N. Nakamura, S. Ujihara, T. Kurosaki, H. Hamaguchi, H. Harada, G. Xia, Y. Morita, I. Aramori, S. Narumiya, S. Sakaguchi, Conversion of antigen-specific effector/memory T cells into Foxp3-expressing Treg cells by inhibition of CDK8/19. *Sci Immunol* **4**, eaaw2707 (2019).

22. Z. C. Poss, C. C. Ebmeier, A. T. Odell, A. Tangpeerachaikul, T. Lee, H. E. Pelish, M. D. Shair, R. D. Dowell, W. M. Old, D. J. Taatjes, Identification of Mediator Kinase Substrates in Human Cells using Cortistatin A and Quantitative Phosphoproteomics. *Cell reports* **15**, 436-450 (2016).

23. W. F. Richter, S. Nayak, J. Iwasa, D. J. Taatjes, The Mediator complex as a master regulator of transcription by RNA polymerase II. *Nat Rev Mol Cell Biol* **23**, 732-749 (2022).

24. O. Luyties, D. J. Taatjes, The Mediator kinase module: an interface between cell signaling and transcription. *Trends Biochem Sci* **47**, 314-327 (2022).

25. M. M. Rinschen, J. Ivanisevic, M. Giera, G. Siuzdak, Identification of bioactive metabolites using activity metabolomics. *Nat Rev Mol Cell Biol* **20**, 353-367 (2019).

26. J. Zhu, C. B. Thompson, Metabolic regulation of cell growth and proliferation. *Nat Rev Mol Cell Biol* **20**, 436-450 (2019).

27. M. D. Galbraith, Z. Andrysik, A. Pandey, M. Hoh, E. A. Bonner, A. A. Hill, K. D. Sullivan, J. M. Espinosa, CDK8 Kinase Activity Promotes Glycolysis. *Cell reports* **21**, 1495-1506 (2017).

28. X. Zhao, D. Feng, Q. Wang, A. Abdulla, X. J. Xie, J. Zhou, Y. Sun, E. S. Yang, L. P. Liu, B. Vaitheesvaran, L. Bridges, I. J. Kurland, R. Strich, J. Q. Ni, C. Wang, J. Ericsson, J. E. Pessin, J. Y. Ji, F. Yang, Regulation of lipogenesis by cyclin-dependent kinase 8-mediated control of SREBP-1. *The Journal of clinical investigation* **122**, 2417-2427 (2012).

29. K. C. Clopper, D. J. Taatjes, Chemical inhibitors of transcription-associated kinases. *Curr Opin Chem Biol* **70**, 102186 (2022).

30. L. Y. Lee, W. M. Oldham, H. He, R. Wang, R. Mulhern, D. E. Handy, J. Loscalzo, Interferon-gamma Impairs Human Coronary Artery Endothelial Glucose Metabolism by Tryptophan Catabolism and Activates Fatty Acid Oxidation. *Circulation* **144**, 1612-1628 (2021).

31. F. Wang, S. Zhang, R. Jeon, I. Vuckovic, X. Jiang, A. Lerman, C. D. Folmes, P. D. Dzeja, J. Herrmann, Interferon Gamma Induces Reversible Metabolic Reprogramming of M1 Macrophages to Sustain Cell Viability and Pro-Inflammatory Activity. *EBioMedicine* **30**, 303-316 (2018).

32. L. Malle, R. S. Patel, M. Martin-Fernandez, O. J. Stewart, Q. Philippot, S. Buta, A. Richardson, V. Barcessat, J. Taft, P. Bastard, J. Samuels, C. Mircher, A. S. Rebillat, L. Maillebouis, M. Vilaire-Meunier, K. Tuballes, B. R. Rosenberg, R. Trachtman, J. L. Casanova, L. D. Notarangelo, S. Gnjatic, D. Bush, D. Bogunovic, Autoimmunity in Down's syndrome via cytokines, CD4 T cells and CD11c(+) B cells. *Nature* **615**, 305-314 (2023).

33. S. Hunter, R. D. Dowell, J. Hendrix, J. Freeman, M. A. Allen, Transcription dosage compensation does not occur in Down syndrome. *bioRxiv* https://doi.org/10.1101/2023.06.07.543933, 2023.2006.2007.543933 (2023).

34. S. Hwang, P. Cavaliere, R. Li, L. J. Zhu, N. Dephoure, E. M. Torres, Consequences of aneuploidy in human fibroblasts with trisomy 21. *Proc Natl Acad Sci U S A* **118** (2021).

35. A. Subramanian, P. Tamayo, V. K. Mootha, S. Mukherjee, B. L. Ebert, M. A. Gillette, A. Paulovich, S. L. Pomeroy, T. R. Golub, E. S. Lander, J. P. Mesirov, Gene set enrichment analysis: a knowledge-based approach for interpreting genome-wide expression profiles. *Proc Natl Acad Sci U S A* **102**, 15545-15550 (2005).

36. K. D. Sullivan, D. Evans, A. Pandey, T. H. Hraha, K. P. Smith, N. Markham, A. L. Rachubinski, K. Wolter-Warmerdam, F. Hickey, J. M. Espinosa, T. Blumenthal, Trisomy 21 causes changes in the circulating proteome indicative of chronic autoinflammation. *Scientific reports* **7**, 14818 (2017).

37. A. Kramer, J. Green, J. Pollard, Jr., S. Tugendreich, Causal analysis approaches in Ingenuity Pathway Analysis. *Bioinformatics* **30**, 523-530 (2014).

38. K. Lambert, K. G. Moo, A. Arnett, G. Goel, A. Hu, K. J. Flynn, C. Speake, A. E. Wiedeman, V. H. Gersuk, P. S. Linsley, C. J. Greenbaum, S. A. Long, R. Partridge, J. H. Buckner, B. Khor, Deep immune phenotyping reveals similarities between aging, Down syndrome, and autoimmunity. *Science translational medicine* **14**, eabi4888 (2022).

39. L. Pecze, E. B. Randi, C. Szabo, Meta-analysis of metabolites involved in bioenergetic pathways reveals a pseudohypoxic state in Down syndrome. *Mol Med* **26**, 102 (2020).

40. R. K. Powers, R. Culp-Hill, M. P. Ludwig, K. P. Smith, K. A. Waugh, R. Minter, K. D. Tuttle, H. C. Lewis, A. L. Rachubinski, R. E. Granrath, M. Carmona-Iragui, R. B. Wilkerson, D. E. Kahn, M. Joshi, A. Lleo, R. Blesa, J. Fortea, A. D'Alessandro, J. C. Costello, K. D. Sullivan, J. M. Espinosa, Trisomy 21 activates the kynurenine pathway via increased dosage of interferon receptors. *Nature communications* **10**, 4766 (2019).

41. D. Sooraj, C. Sun, A. Doan, D. J. Garama, M. V. Dannappel, D. Zhu, H. K. Chua, S. Mahara, W. A. Wan Hassan, Y. K. Tay, A. Guanizo, D. Croagh, Z. Prodanovic, D. J. Gough, C. Wan, R. Firestein, MED12 and BRD4 cooperate to sustain cancer growth upon loss of mediator kinase. *Mol Cell* **82**, 123-139 e127 (2022).

42. Z. Andrysik, H. Bender, M. D. Galbraith, J. M. Espinosa, Multi-omics analysis reveals contextual tumor suppressive and oncogenic gene modules within the acute hypoxic response. *Nature communications* **12**, 1375 (2021).

43. K. A. Audetat, M. D. Galbraith, A. T. Odell, T. Lee, A. Pandey, J. M. Espinosa, R. D. Dowell, D. J. Taatjes, A Kinase-Independent Role for Cyclin-Dependent Kinase 19 in p53 Response. *Mol Cell Biol* **37**, e00626-00616 (2017).

44. M. C. Basil, B. D. Levy, Specialized pro-resolving mediators: endogenous regulators of infection and inflammation. *Nature reviews. Immunology* **16**, 51-67 (2016).

45. A. S. Husted, M. Trauelsen, O. Rudenko, S. A. Hjorth, T. W. Schwartz, GPCR-Mediated Signaling of Metabolites. *Cell metabolism* **25**, 777-796 (2017).

46. P. M. Jordan, O. Werz, Specialized pro-resolving mediators: biosynthesis and biological role in bacterial infections. *The FEBS journal* **289**, 4212-4227 (2022).

47. I. Kimura, A. Ichimura, R. Ohue-Kitano, M. Igarashi, Free Fatty Acid Receptors in Health and Disease. *Physiol Rev* **100**, 171-210 (2020).

48. M. Alhouayek, G. G. Muccioli, COX-2-derived endocannabinoid metabolites as novel inflammatory mediators. *Trends Pharmacol Sci* **35**, 284-292 (2014).

49. J. Fu, S. Gaetani, F. Oveisi, J. Lo Verme, A. Serrano, F. Rodriguez De Fonseca, A. Rosengarth, H. Luecke, B. Di Giacomo, G. Tarzia, D. Piomelli, Oleylethanolamide regulates feeding and body weight through activation of the nuclear receptor PPAR-alpha. *Nature* **425**, 90-93 (2003).

50. L. Yang, H. Guo, Y. Li, X. Meng, L. Yan, Z. Dan, S. Wu, H. Zhou, L. Peng, Q. Xie, X. Jin, Oleoylethanolamide exerts anti-inflammatory effects on LPS-induced THP-1 cells by enhancing PPARalpha signaling and inhibiting the NF-kappaB and ERK1/2/AP-1/STAT3 pathways. *Scientific reports* **6**, 34611 (2016).

51. C. A. Dinarello, Historical insights into cytokines. *Eur J Immunol* **37 Suppl 1**, S34-45 (2007).

52. M. M. Scotti, M. S. Swanson, RNA mis-splicing in disease. *Nature reviews. Genetics* **17**, 19-32 (2016).

53. S. Shen, J. W. Park, Z. X. Lu, L. Lin, M. D. Henry, Y. N. Wu, Q. Zhou, Y. Xing, rMATS: robust and flexible detection of differential alternative splicing from replicate RNA-Seq data. *Proc Natl Acad Sci U S A* **111**, E5593-5601 (2014).

54. S. Schoors, U. Bruning, R. Missiaen, K. C. Queiroz, G. Borgers, I. Elia, A. Zecchin, A. R. Cantelmo, S. Christen, J. Goveia, W. Heggermont, L. Godde, S. Vinckier, P. P. Van Veldhoven, G. Eelen, L. Schoonjans, H. Gerhardt, M. Dewerchin, M. Baes, K. De Bock, B. Ghesquiere, S. Y. Lunt, S. M. Fendt, P. Carmeliet, Fatty acid carbon is essential for dNTP synthesis in endothelial cells. *Nature* **520**, 192-197 (2015).

55. M. Baker, M. Petasny, N. Taqatqa, M. Bentata, G. Kay, E. Engal, Y. Nevo, A. Siam, S. Dahan, M. Salton, KDM3A regulates alternative splicing of cell-cycle genes following DNA damage. *RNA* **27**, 1353-1362 (2021).

56. A. Gautam, R. J. Grainger, J. Vilardell, J. D. Barrass, J. D. Beggs, Cwc21p promotes the second step conformation of the spliceosome and modulates 3' splice site selection. *Nucleic Acids Res* **43**, 3309-3317 (2015).

57. S. Soucek, Y. Zeng, D. L. Bellur, M. Bergkessel, K. J. Morris, Q. Deng, D. Duong, N. T. Seyfried, C. Guthrie, J. P. Staley, M. B. Fasken, A. H. Corbett, The Evolutionarily-conserved Polyadenosine RNA Binding Protein, Nab2, Cooperates with Splicing Machinery to Regulate the Fate of pre-mRNA. *Mol Cell Biol* **36**, 2697-2714 (2016).

58. X. Rambout, F. Dequiedt, L. E. Maquat, Beyond Transcription: Roles of Transcription Factors in Pre-mRNA Splicing. *Chemical reviews* **118**, 4339-4364 (2018).

59. M. Maceyka, S. Spiegel, Sphingolipid metabolites in inflammatory disease. *Nature* **510**, 58-67 (2014).

60. J. Y. L. Chiang, J. M. Ferrell, Bile Acids as Metabolic Regulators and Nutrient Sensors. *Annu Rev Nutr* **39**, 175-200 (2019).

61. A. Roy, M. Kundu, M. Jana, R. K. Mishra, Y. Yung, C. H. Luan, F. J. Gonzalez, K. Pahan, Identification and characterization of PPARalpha ligands in the hippocampus. *Nature chemical biology* **12**, 1075-1083 (2016).

62. N. J. Spann, L. X. Garmire, J. G. McDonald, D. S. Myers, S. B. Milne, N. Shibata, D. Reichart, J. N. Fox, I. Shaked, D. Heudobler, C. R. Raetz, E. W. Wang, S. L. Kelly, M. C. Sullards, R. C. Murphy, A. H. Merrill, Jr., H. A. Brown, E. A. Dennis, A. C. Li, K. Ley, S. Tsimikas, E. Fahy, S. Subramaniam, O. Quehenberger, D. W. Russell, C. K. Glass, Regulated accumulation of desmosterol integrates macrophage lipid metabolism and inflammatory responses. *Cell* **151**, 138-152 (2012).

63. Y. Sun, A. Bennett, Cannabinoids: a new group of agonists of PPARs. *PPAR Res* **2007**, 23513 (2007).

64. C. Yang, J. G. McDonald, A. Patel, Y. Zhang, M. Umetani, F. Xu, E. J. Westover, D. F. Covey, D. J. Mangelsdorf, J. C. Cohen, H. H. Hobbs, Sterol intermediates from cholesterol biosynthetic pathway as liver X receptor ligands. *J Biol Chem* **281**, 27816-27826 (2006).

65. J. R. Schultz, H. Tu, A. Luk, J. J. Repa, J. C. Medina, L. Li, S. Schwendner, S. Wang, M. Thoolen, D. J. Mangelsdorf, K. D. Lustig, B. Shan, Role of LXRs in control of lipogenesis. *Genes Dev* **14**, 2831-2838 (2000).

66. K. D. Tuttle, K. A. Waugh, P. Araya, R. Minter, D. J. Orlicky, M. Ludwig, Z. Andrysik, M. A. Burchill, B. A. J. Tamburini, C. Sempeck, K. Smith, R. Granrath, D. Tracy, J. Baxter, J. M. Espinosa, K. D. Sullivan, JAK1 Inhibition Blocks Lethal Immune Hypersensitivity in a Mouse Model of Down Syndrome. *Cell reports* **33**, 108407 (2020).

67. L. Ford, A. D. Kennedy, K. D. Goodman, K. L. Pappan, A. M. Evans, L. A. D. Miller, J. E. Wulff, B. R. Wiggs, J. J. Lennon, S. Elsea, D. R. Toal, Precision of a Clinical Metabolomics Profiling Platform for Use in the Identification of Inborn Errors of Metabolism. *J Appl Lab Med* **5**, 342-356 (2020).

68. C. D. Dehaven, A. M. Evans, H. Dai, K. A. Lawton, Organization of GC/MS and LC/MS metabolomics data into chemical libraries. *Journal of cheminformatics* **2**, 9 (2010).

69. D. Kim, J. M. Paggi, C. Park, C. Bennett, S. L. Salzberg, Graph-based genome alignment and genotyping with HISAT2 and HISAT-genotype. *Nat Biotechnol* **37**, 907-915 (2019).

70. Y. Liao, G. K. Smyth, W. Shi, featureCounts: an efficient general purpose program for assigning sequence reads to genomic features. *Bioinformatics* **30**, 923-930 (2014).

71. S. Anders, W. Huber, Differential expression analysis for sequence count data. *Genome biology* **11**, R106 (2010).

72. M. Ashburner, C. A. Ball, J. A. Blake, D. Botstein, H. Butler, J. M. Cherry, A. P. Davis, K. Dolinski, S. S. Dwight, J. T. Eppig, M. A. Harris, D. P. Hill, L. Issel-Tarver, A. Kasarskis, S.

Lewis, J. C. Matese, J. E. Richardson, M. Ringwald, G. M. Rubin, G. Sherlock, Gene ontology: tool for the unification of biology. The Gene Ontology Consortium. *Nature genetics* **25**, 25-29 (2000).

73. S. Y. Lunt, M. G. Vander Heiden, Aerobic glycolysis: meeting the metabolic requirements of cell proliferation. *Annu Rev Cell Dev Biol* **27**, 441-464 (2011).

74. R. G. Jones, E. J. Pearce, MenTORing Immunity: mTOR Signaling in the Development and Function of Tissue-Resident Immune Cells. *Immunity* **46**, 730-742 (2017).

75. C. F. Lee, R. E. Carley, C. A. Butler, A. R. Morrison, Rac GTPase Signaling in Immune-Mediated Mechanisms of Atherosclerosis. *Cells* **10** (2021).

Figures
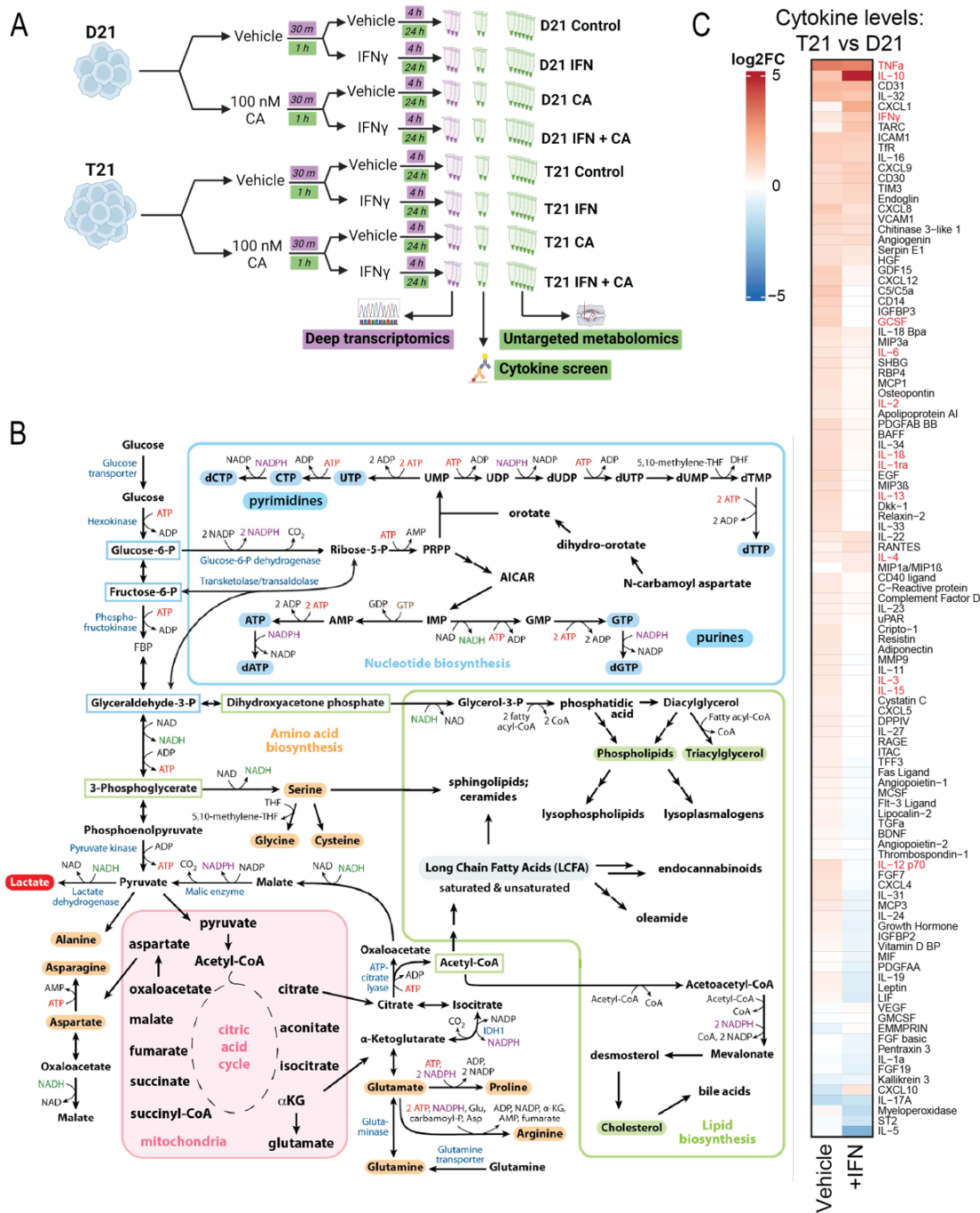
Figure 1

Fig 1. Experimental overview; elevated cytokines in T21 cells. (A) Schematic of cell treatment and data collection workflow for metabolomics, cytokine screen (green shading) and RNA-seq (purple shading). Created with Biorender.com. **(B)** Simplified diagram of human metabolic pathways, with an emphasis on those relevant to this study. Figure adapted from (73). **(C)** Heatmap of all cytokines measured (n = 105), comparing relative levels in vehicle-treated T21 cells vs. vehicle-treated D21 cells (left column) and relative levels in IFNγ-treated T21 cells vs. IFNγ-treated D21 cells (right column). Note elevated cytokine levels in T21 cells under basal conditions, whereas levels become more equivalent in +IFNγ conditions, similar to gene expression results (RNA-seq) shown in **Figure S4**.
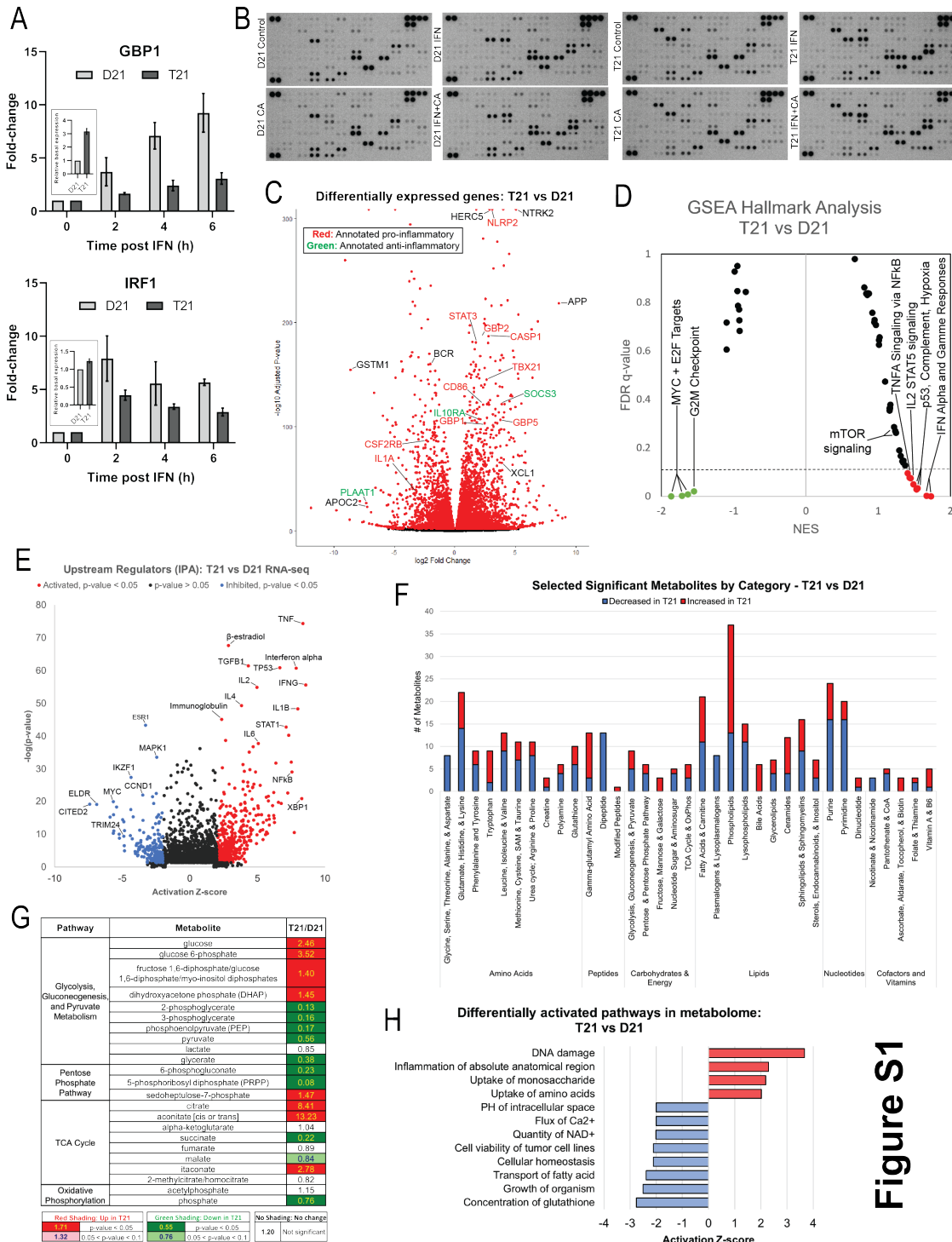
Figure S1. Comparisons between T21 and D21 cells. (A) Time course of relative gene expression levels measured by real-time quantitative PCR (RT-qPCR) of GBP1 and IRF1, two interferon stimulated genes, following treatment with 10 ng/mL IFNγ compared to untreated cells. Data normalized to expression of GAPDH and represented as mean ± SD from two independent experiments. Inset panel represents relative basal expression of each gene in untreated T21 cells compared to untreated D21 cells. **(B)** Representative data from cytokine protein arrays. Arrays were incubated with cell lysates (250 µg total protein) treated as shown. Multiple exposures were taken to ensure that every spot was measured in the linear range; duplicate spots were averaged. Averaged intensity values from two biological replicates/condition were analyzed using ANOVA. **(C)** Volcano plot of differentially expressed genes in T21 cells compared to D21; selected genes

are color-coded based on proinflammatory (red), anti-inflammatory (green), or other (black) roles in IFN signaling. Genes represented by red dots have an adjusted p-value of <0.01. **(D)** GSEA moustache plot of Hallmark pathways comparing T21 cells with D21. **(E)** Ingenuity Pathway Analysis of upstream regulators predicted to be responsible for differential transcription in T21 cells compared to D21 cells. Analysis used genes >1.25x up- or down-regulated, with an adjusted p-value <0.1. List of regulators was filtered to exclude drugs or other exogenous compounds. **(F)** Differential metabolites summary (ANOVA p-value <0.1) in untreated T21 cells relative to untreated D21 cells, broken down by category; excludes unknown and xenobiotic metabolites. **(G)** Relative levels of metabolites from core metabolic pathways in untreated T21 cells compared with untreated D21 cells. **(H)** Selected results of pathway analysis based on metabolite levels in untreated T21 compared with D21 cells, using the "Diseases & Functions" list from Ingenuity Pathway Analysis.
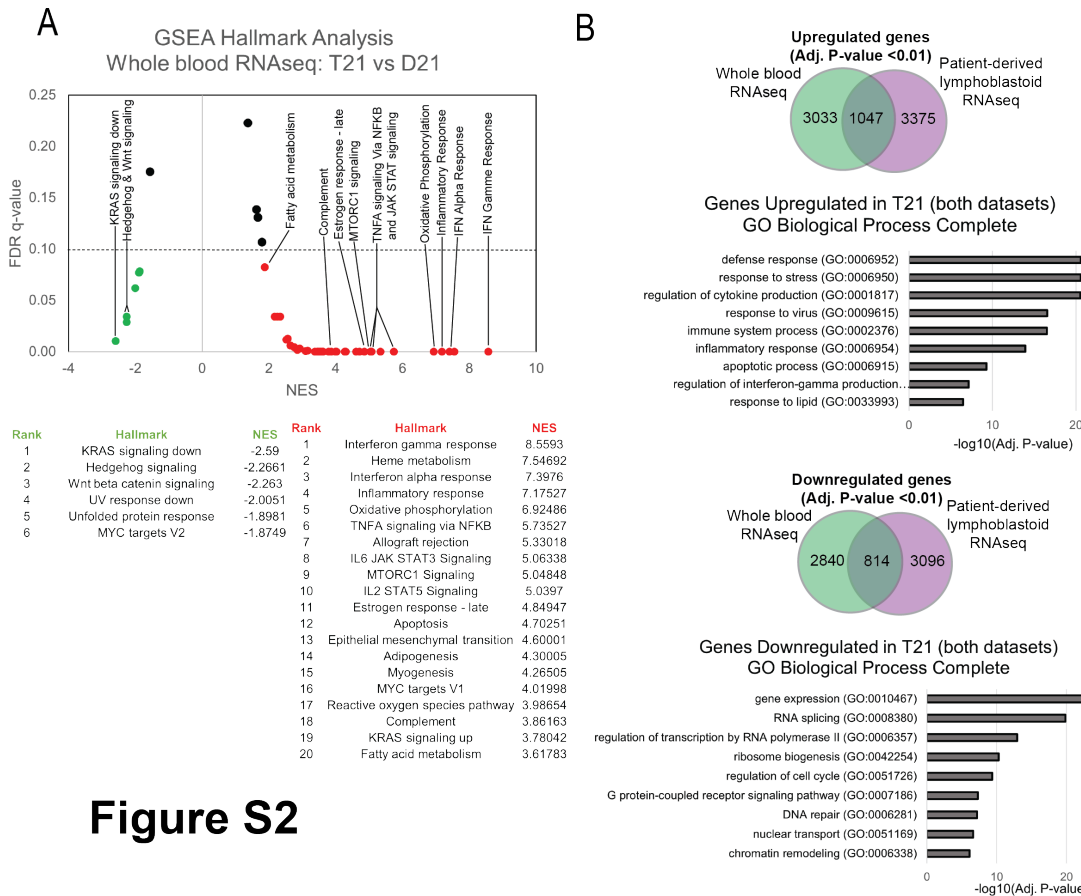
Figure S2. Data comparison with whole blood cohort clinical studies. (A) GSEA moustache plot of Hallmark pathway activation in whole blood samples from a cohort study of T21 individuals compared to euploid controls (11). **(B)** Venn diagram of upregulated or downregulated genes (adjusted p-value <0.01) in Trisomy 21 from this study and in whole blood samples from the cohort study (NCT02864108). Genes either up- or down-regulated in both studies were analyzed using Gene Ontology Enrichment Analysis with the GO aspect "Biological Processes."

A RNA-seq CA vs Ctrl

B IPA upstream regulators T21 CA vs. Ctrl

Factor	Z-score	Description
SREBF1	5.335	TF; fatty acid and cholesterol biosynthesis
SCAP	5.149	SREBP processing/activation
SREBF2	4.959	TF; fatty acid and cholesterol biosynthesis
INSR	3.308	Insulin receptor; glucose/lipid homeostasis
PPARGC1B	3.044	PGC1β; PPAR co-activator; fat metabolism
NR1H3	2.833	LXRα; lipid homeostasis and inflammation
MBTPS1	2.646	TF protease; FA & cholesterol homeostasis
ACSS2	2.449	Acyl CoA synthetase; lipid biosynthesis
DBI	2.449	PPAR signaling; lipid metabolism
CYP7A1	2.433	converts cholesterol --> bile acids
CEBPA	2.314	lipid homeostasis; co-act w/ SREBP TFs
FASN	2.157	fatty acid synthase
ELOVL5	-2.623	elongation of PUFAs
ACACB	-2.425	FA synthesis; (−) reg'n of FA oxidation
ACSL4	-2.425	FA oxidation enzyme
CETP	-2.236	cholesterol export
CYP51A1	-2.236	lipid biosynthesis enzyme
FDFT1	-2.213	squalene synthase; cholesterol biosynthesis
ANGPTL3	-2	lipid metabolism
ANGPTL8	-2	lipid metabolism

C LCFAs (CAvsCtrl) Endocannabinoids (CAvsCtrl)

D

PUFAs

eicosapentaenoic acid (EPA)

docosahexaenoic acid (DHA)

oleic acid

GPCRs (e.g. FFAR1, FFAR4, GPR119)

oleamide ⊣ NFκB

β-arrestin → Inflammasome activation

OEA

Endocannabinoids   Desmosterol

PPARs   LXRs

Anti-inflammatory gene expression

E Cytokine levels: CA vs Control

TNFa, IL-10, Relaxin-2, * Dkk-1, * BDNF, CXCL10, GMCSF, MIF, IL-33, IL-34, IL-32, IFNgamma, MIP3ß, IL-2, IL-17A, RANTES, IL-18 Bpa, DPPIV, GCSF, TARC, IL-3, MIP1a/MIP1ß, CXCL9

log2FC

Outlined tile: FC >1.5 or <0.75
* indicates p-value <0.1

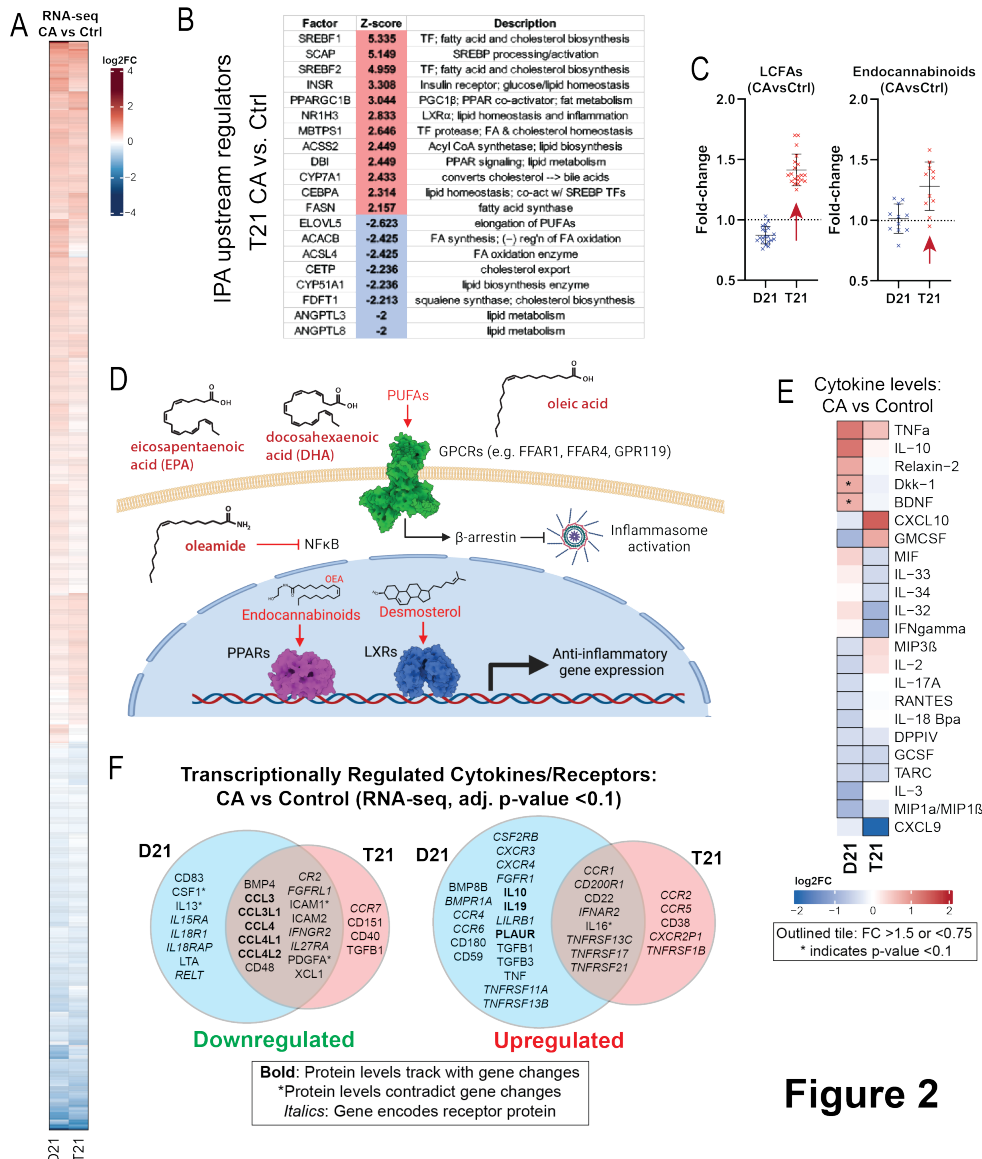**F** Transcriptionally Regulated Cytokines/Receptors: CA vs Control (RNA-seq, adj. p-value <0.1)

D21: CD83, CSF1*, IL13*, IL15RA, IL18R1, IL18RAP, LTA, RELT

(shared): BMP4, **CCL3**, **CCL3L1**, **CCL4**, **CCL4L1**, **CCL4L2**, CD48

T21: CR2, FGFRL1, ICAM1*, ICAM2, IFNGR2, IL27RA, PDGFA*, XCL1

CCR7, CD151, CD40, TGFB1

D21: BMP8B, BMPR1A, CCR4, CCR6, CD180, CD59

(shared): CSF2RB, CXCR3, CXCR4, FGFR1, **IL10**, **IL19**, **LILRB1**, **PLAUR**, TGFB1, TGFB3, TNF, TNFRSF11A, TNFRSF13B

T21: CCR1, CD200R1, CD22, IFNAR2, IL16*, TNFRSF13C, TNFRSF17, TNFRSF21

CCR2, CCR5, CD38, CXCR2P1, TNFRSF1B

Downregulated   **Upregulated**

Bold: Protein levels track with gene changes
*Protein levels contradict gene changes
Italics: Gene encodes receptor protein

Figure 2

Fig 2. Mediator kinase inhibition tempers inflammatory pathways under basal conditions, T21-specific effects. (A) Heatmap of genes with differential expression in D21 or T21 cells treated with CA (100 nM) compared to DMSO control cells. Only genes with adjusted p-value <0.01 in one or both cell lines are shown. **(B)** Table of activation Z-scores for selected upstream regulators predicted for gene expression changes in CA-treated T21 cells relative to vehicle controls. This curated set emphasizes lipid metabolite changes triggered by Mediator kinase inhibition. **(C)** Box plots showing relative levels of selected lipid metabolites in CA-treated D21 and T21 cells compared to DMSO controls. CA-dependent changes in LCFA and endocannabinoids (arrows) are consistent with anti-inflammatory effects (see text). **(D)** Simplified diagram of pathways through which selected lipid metabolites regulate inflammation. **(E)** Heatmap of average relative cytokine levels in CA-treated cells compared to DMSO controls. Only cytokines with relative levels of ≥1.5 (log2FC; red shading) or ≤0.75 (blue shading) in one or both cell lines are shown; cytokines meeting this threshold are outlined in black. Cytokines with an asterisk (*) had an adjusted p-value <0.1 using ANOVA. **(F)** Venn diagrams of cytokines and cytokine receptor genes (in *italics*) that were downregulated (FC <0.8, left diagram) or upregulated (FC >1.2, right diagram) in CA-treated D21 and T21 cells, compared to DMSO controls. Cytokines with matching trends from RNA-seq (4h) are listed in bold, whereas cytokines with inverse trends in at least one cell type are marked with an asterisk.
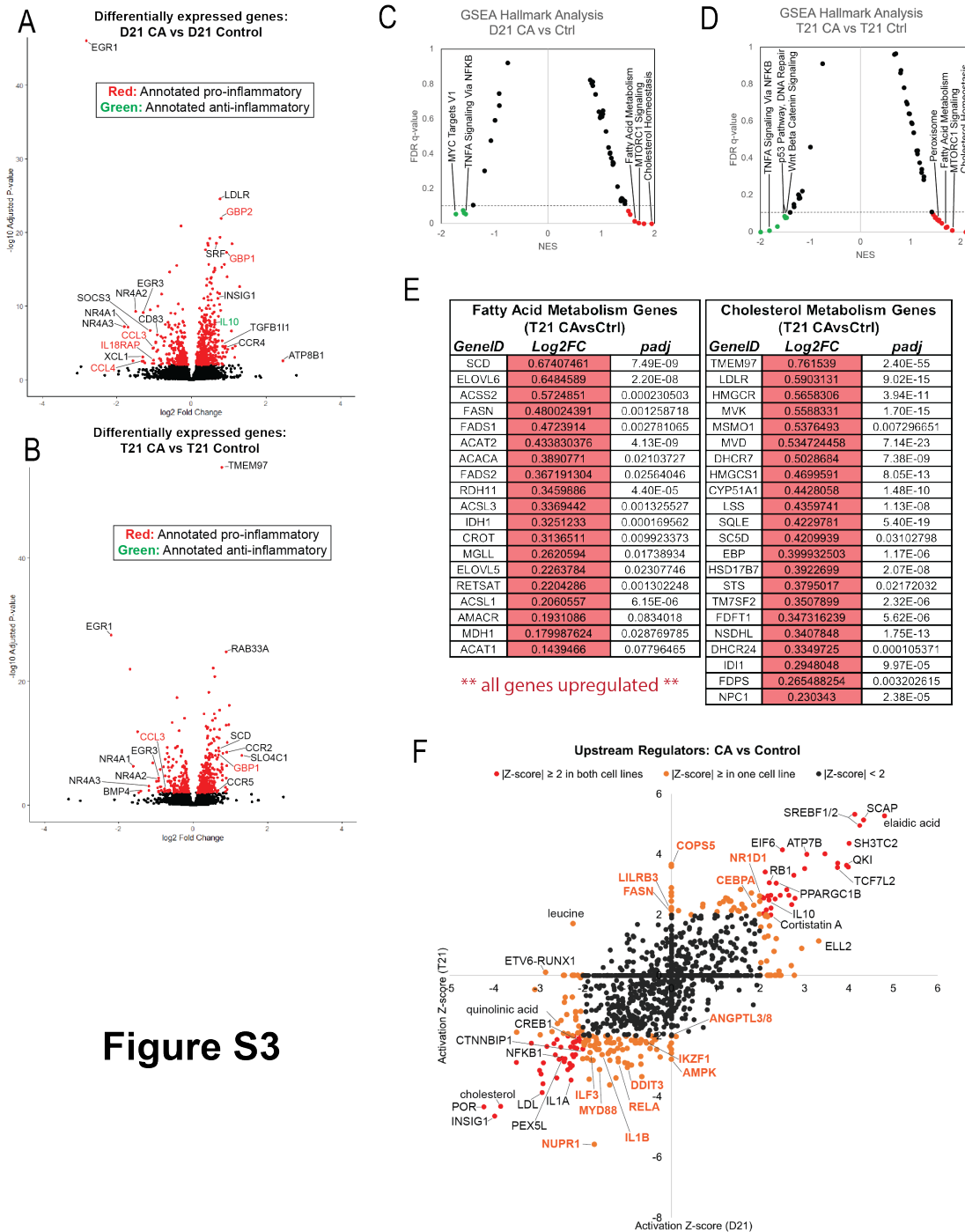
26

Figure S3

Figure S3. CA suppresses T21 inflammatory pathways under basal conditions. (A, B) Volcano plots showing differentially expressed genes following CA treatment in D21 (A) or T21 (B) cells, with selected genes color-coded based on pro-inflammatory (red), anti-inflammatory (green) roles. Genes represented by red dots have an adjusted p-value of <0.01. **(C, D)** GSEA moustache plots of Hallmark pathway activation in CA-treated D21 (C) and T21 (D) cells compared to DMSO controls. **(E)** Tables of genes involved in fatty acid metabolism (left) or cholesterol metabolism (right) that are differentially expressed (adjusted p-value ≤ 0.1) in CA-treated T21 cells relative to vehicle controls, showing consistent upregulation in both pathways. **(F)** Ingenuity Pathway Analysis of upstream regulators predicted for differential gene expression (RNA-seq) in CA-treated D21 and T21 cells compared to DMSO controls. Predicted regulators specific for T21 cells are labeled in orange font. Analysis used genes with an adjusted p-value <0.1. List of regulators was filtered to exclude drugs or other exogenous compounds, with the exception of Cortistatin A.
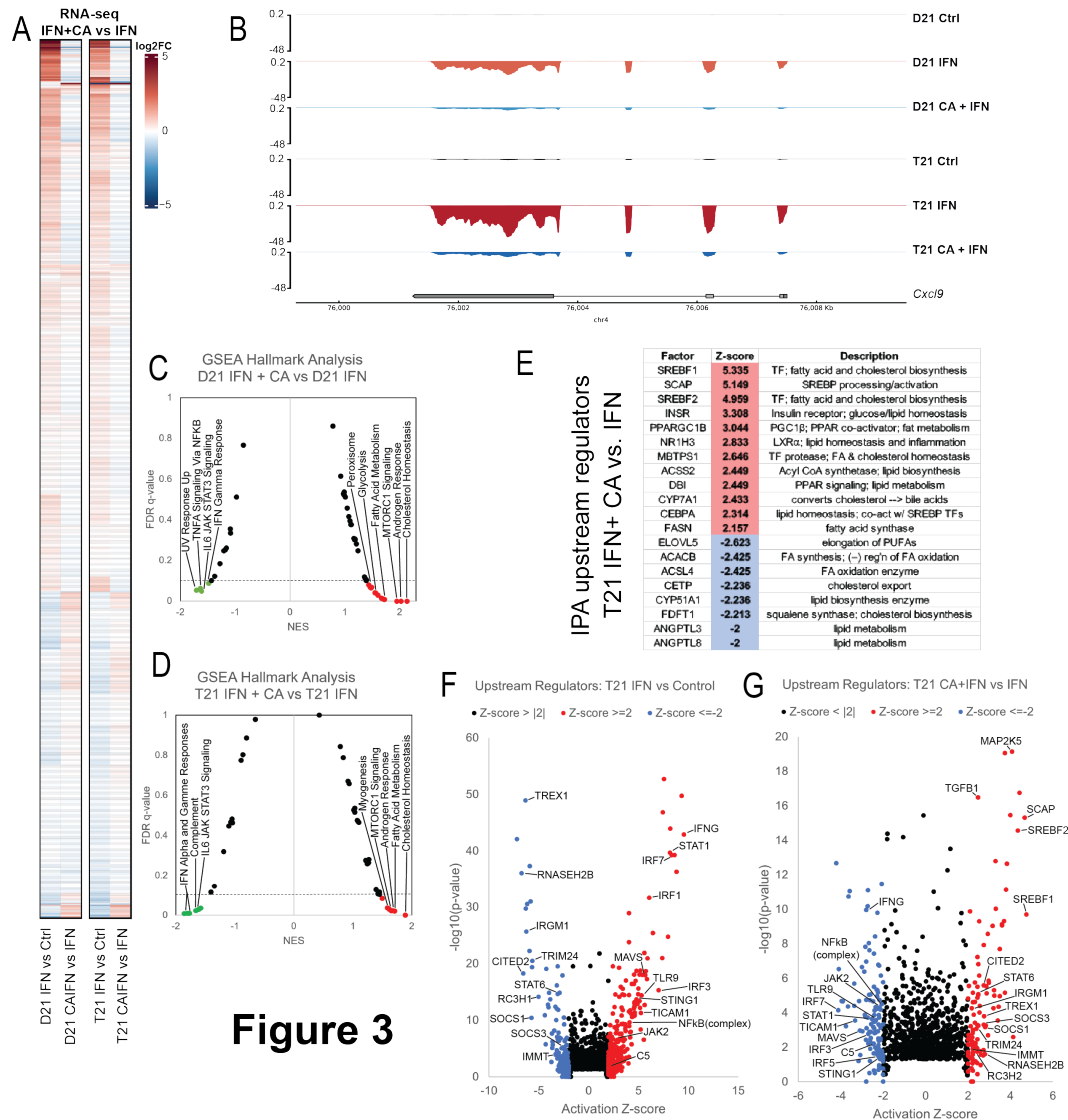
Figure 3

Fig 3. Mediator kinase inhibition antagonizes IFNγ transcriptional responses in T21 and D21. (A) Heatmap comparing gene expression patterns (RNA-seq) in IFNγ-treated D21 or T21 cells ±CA. This comparison exposes the CA-specific effects during IFNγ stimulation, which broadly counter changes caused by IFNγ alone. Genes with statistically significant (adjusted p-value <0.01) levels in one or both cell lines in IFNγ vs. control comparisons are shown. **(B)** Representative genome browser tracks for CXCL9 locus in D21 and T21 cells treated with vehicle, IFNγ, or IFNγ +CA, showing both IFNγ-dependent induction and CA-dependent suppression of transcription. **(C, D)** GSEA moustache plots of Hallmark pathways in D21 (C) and T21 (D) cells treated with IFNγ +CA compared to IFNγ alone. This exposes CA-specific effects during IFNγ stimulation; note the CA-dependent repression of gene sets associated with inflammatory signaling pathways. **(E)** Table of activation Z-scores for selected upstream regulators predicted for gene expression changes in CA-treated T21 cells treated with IFNγ +CA relative to IFNγ alone. This curated set emphasizes lipid metabolite changes triggered upon Mediator kinase inhibition. **(F, G)** Ingenuity Pathway Analysis upstream regulators results from comparison of differential gene expression (RNA-seq) in T21 cells during IFNγ treatment (F) or in cells treated with IFNγ +CA compared to IFNγ alone (G). Selected TFs and other factors associated with inflammatory responses are labeled. Note prominent activation of pro-inflammatory TFs in +IFNγ cells (F), whereas these same TFs are predicted to be repressed in CA-treated cells (G). Analysis used only genes with an adjusted p-value <0.1.
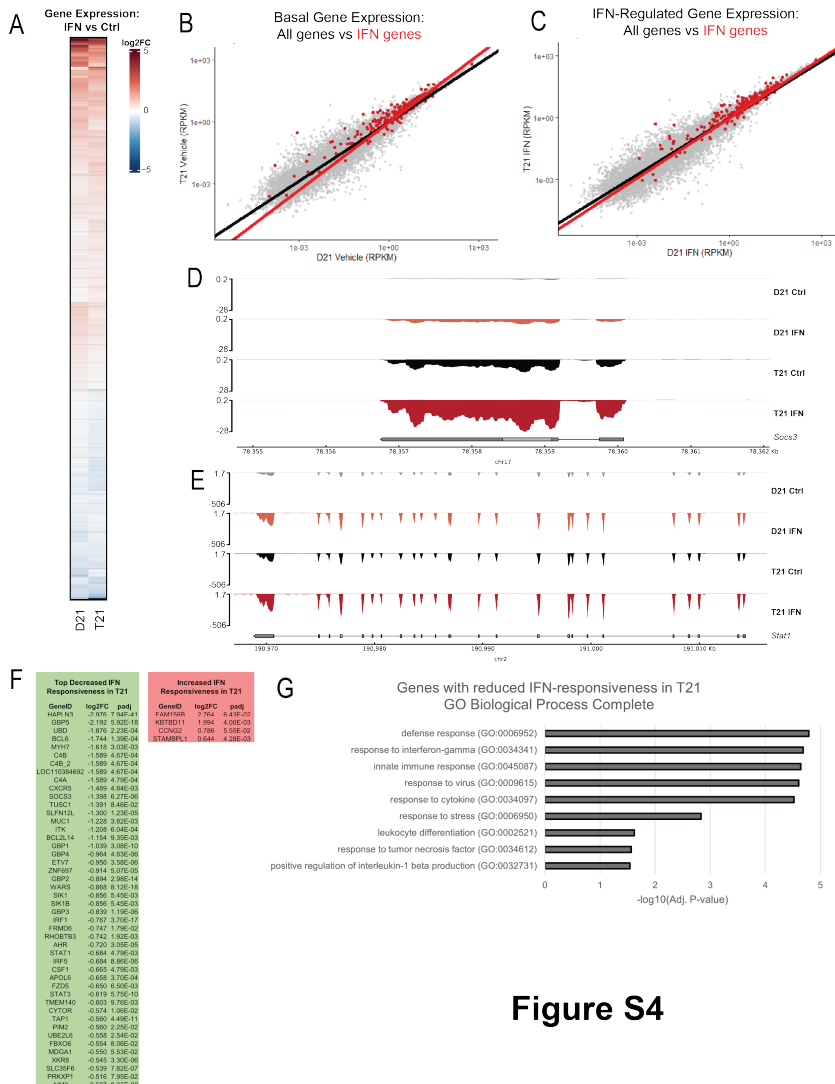
28

Figure S4

Figure S4. The response to exogenous IFNγ is suppressed in T21 vs. D21 cells. (A) Heatmap of genes with differential expression in D21 or T21 cells treated with IFNγ compared to controls. Genes with adjusted p-value <0.01 in one or both cell lines are shown. **(B)** Average values across biological replicates for reads per kilobase of transcript, per million mapped reads (RPKM) in vehicle-treated D21 cells (x-axis) and vehicle-treated T21 cells (y-axis). Gray dots represent all genes with an RPKM value >0, and red dots represent genes from the GSEA Hallmarks IFNγ and IFNα signaling pathways. Linear regression trendlines for each set are depicted as follows; black: all genes; red: IFN response genes. The greater slope for IFN-responsive genes indicates higher basal expression of these genes in T21 cells. **(C)** Similar to panel B, except in IFNγ-treated D21 (x-axis) and IFNγ-treated T21 cells (y-axis). Note the linear regression trendlines are more similar under IFNγ-stimulation conditions, compared with basal conditions (panel B), which provides evidence for dampened IFNγ transcriptional response in T21 cells, likely from higher basal level expression, such that gene expression ends up being similar in T21 and D21 cells treated with exogenous IFNγ. **(D, E)** Representative genome browser tracks (RNA-seq data) for SOCS3 (D) or STAT1 (E) in D21 and T21 cells ± IFNγ treatment. **(F)** Genes with lower (green) or higher (red) relative expression in IFNγ-treated T21 cells (vs IFNγ-treated D21; adjusted p-value <0.1). Only genes with a log2FC ≥ l0.5l are shown. **(G)** Gene Ontology Enrichment Analysis with the GO aspect "Biological Processes" for genes with reduced responsiveness to IFNγ stimulation in T21 cells. Many genes with reduced expression in T21 cells represent inflammatory pathways, consistent with a suppressed response to exogenous IFNγ in T21 cells, vs D21.
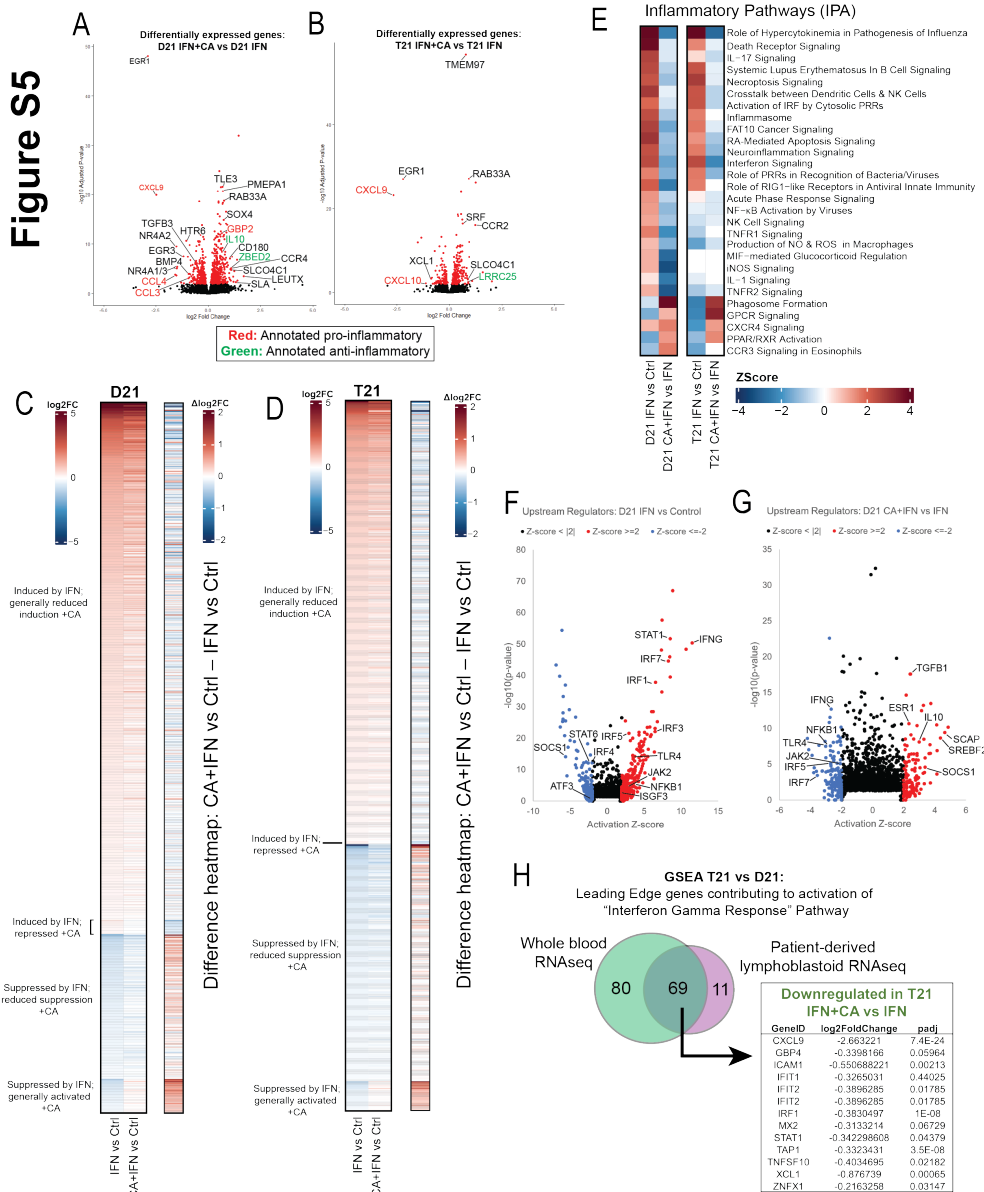
29

Figure S5. Mediator kinase inhibition antagonizes IFNγ transcriptional responses. (A, B) Volcano plots of differentially expressed genes in IFNγ-treated cells ±CA in D21 (A) or T21 (B) cells. Names of selected genes are color-coded based on proinflammatory (red) or anti-inflammatory (green) roles. Genes represented by red dots have an adjusted p-value of <0.01. **(C, D)** Heatmaps and "difference" heatmaps based upon RNA-seq data under various conditions in D21 (C) or T21 (D) cells. At left (panel C, D), heatmaps represent all genes with an adjusted p-value <0.01 in IFNγ vs. Control comparisons for each cell line. Log2FC values were used to sort genes by expression trends in D21 and T21 cells. Data for IFNγ +CA vs. Ctrl are shown alongside IFNγ vs. Ctrl to better visualize CA-dependent effects. For difference heatmaps (at right in panel C, D), Log2FC values for each gene in the IFNγ vs. Control comparison were subtracted from Log2FC values for CA+IFNγ vs. Control comparisons to generate "difference" Log2FC values, which are shown in the difference heatmap on the right. **(E)** Heatmaps showing inflammatory pathways in the Ingenuity Pathway Analysis "Diseases & Functions" list, generated from RNA-seq data. Heatmaps show pathway activation in IFNγ vs. Control compared to IFNγ+CA vs. IFNγ in both D21 and T21 cells, to focus on CA-dependent effects during IFNγ response. **(F, G)** Volcano plots from IPA upstream regulators results, derived from differential gene expression (RNA-seq) in D21 cells during IFNγ treatment (F) or in cells treated with IFNγ +CA compared to IFNγ alone (G).

30

Selected TFs and other factors associated with inflammatory responses are labeled. Note prominent activation of pro-inflammatory TFs in +IFNγ cells (F), whereas these same TFs are predicted to be repressed in CA-treated cells (G). Analysis used only genes with an adjusted p-value <0.1. **(H)** Venn diagram showing overlap of leading edge genes in the GSEA "Interferon Gamma Response" pathway based upon RNA-seq data from a T21 vs. D21 whole blood cohort study (11) and RNA-seq data from the sibling-matched T21 vs. D21 cells in this study. A substantial number of genes with the IFN "leading edge" designation in this study (i.e. increased expression in T21 vs. D21; 69 out of 80) were shared among the whole blood clinical cohort study; these 69 genes were down-regulated by CA treatment in T21 cells. A partial list of these genes is shown, with Log2FC and adjusted p-values.
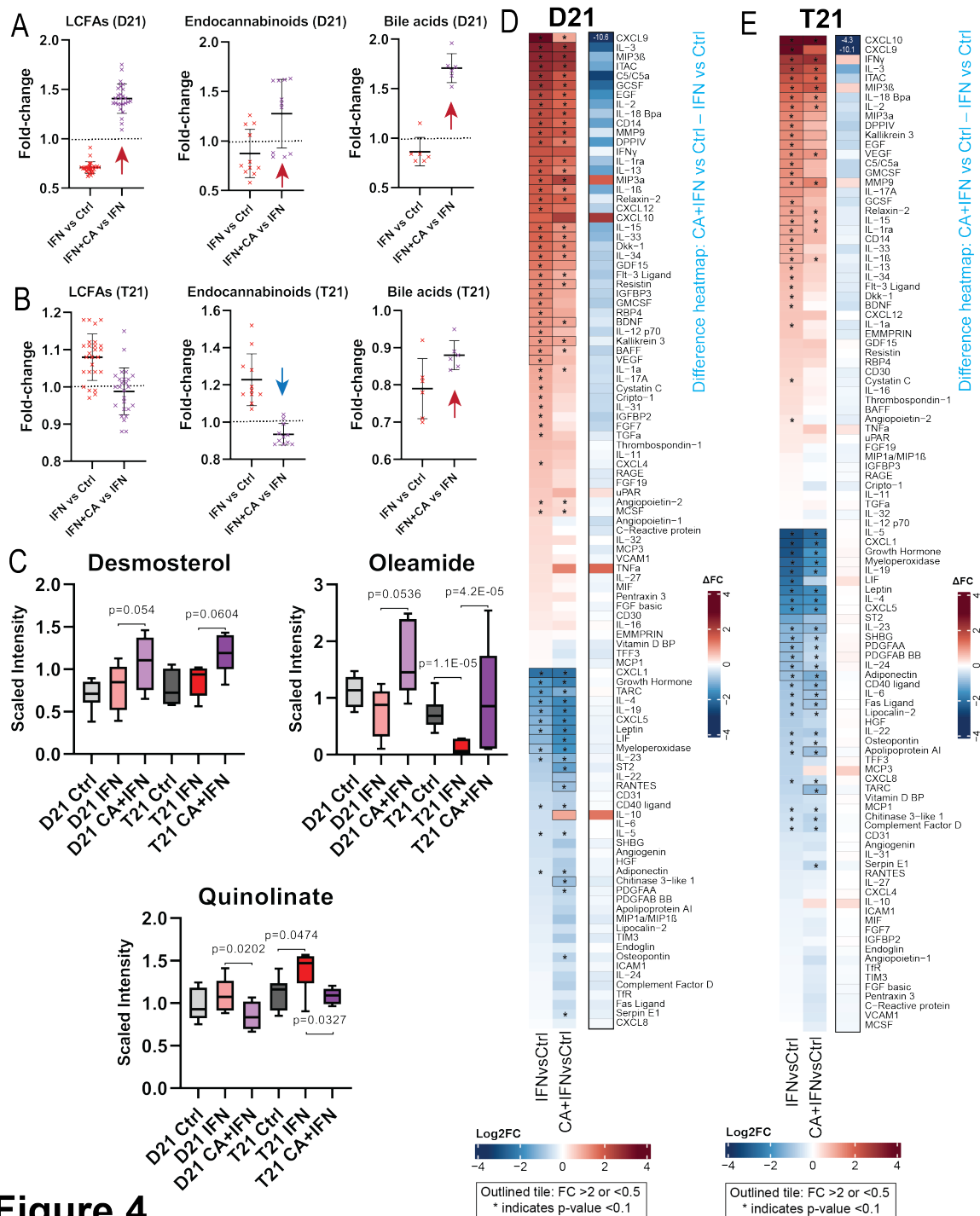
Figure 4

Fig 4. Mediator kinase inhibition reverses pro-inflammatory metabolic and cytokine changes triggered by IFNγ. (A, B) Effect of IFNγ treatment on select classes of lipid metabolites is shown (IFNγ vs. Ctrl) alongside the effect of CA treatment in IFNγ-treated cells, in D21 (B) and T21 (B) cells. The LCFAs represented here include saturated, mono- and poly-unsaturated FA, shown in rows 3-28 in **Supplementary Table 9**. Each point represents a different metabolite, with line and whiskers representing the mean and SD. Note that CA treatment reverses IFNγ effects generally across these sets of metabolites (arrows). **(C)** Box plots showing levels of anti-inflammatory metabolites desmosterol or oleamide, and pro-inflammatory metabolite quinolinate, in D21 or T21 cells treated with vehicle (Ctrl), IFNγ, or IFNγ +CA. **(D, E)** Heatmaps showing changes in cytokine levels in D21 (D) and T21 (E) cells, after the indicated treatments. Only cytokines with relative

levels of ≥2.0 (log2FC; red shading) or ≤0.5 (blue shading) in one or both cell lines are shown; cytokines meeting this threshold are outlined in black. Cytokines with an asterisk (*) had an adjusted p-value <0.1 using ANOVA. Alongside each heatmap set (D21 or T21) is a "difference" heatmap (IFN+CA vs. Ctrl – IFN vs. Ctrl levels) that highlights how Mediator kinase inhibition suppresses cytokine responses to IFNγ. For example, note how most cytokines whose levels increase +IFNγ show generally reduced levels in IFN+CA conditions (majority blue in difference heatmap).
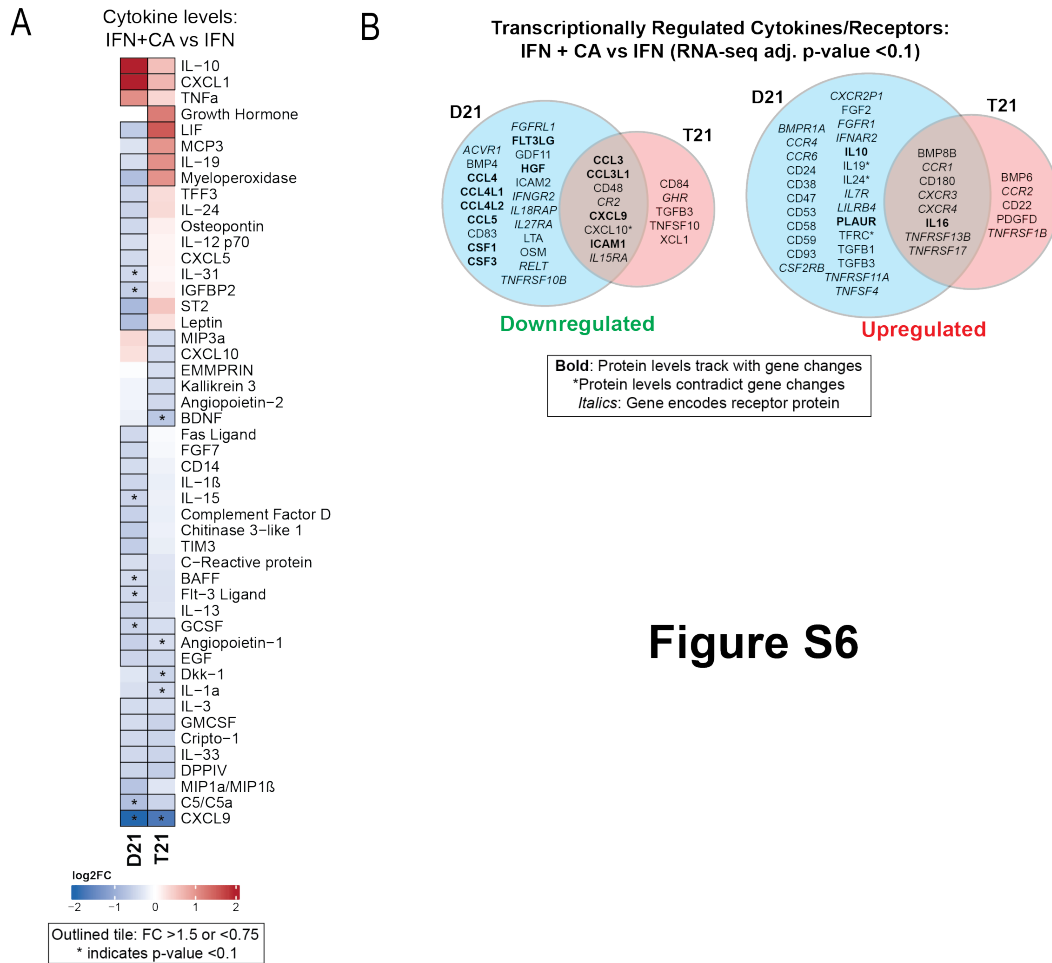
Figure S6

Figure S6. Mediator kinases transcriptionally enable cytokine responses to IFNγ. (A) Heatmap of average relative cytokine levels in cells treated with IFNγ +CA compared to IFNγ alone. Only cytokines with relative levels of ≥1.5 (log2FC; red shading) or ≤0.75 (blue shading) in one or both cell lines are shown; cytokines meeting this threshold are outlined in black. Cytokines with an asterisk (*) had an adjusted p-value <0.1 using ANOVA. **(B)** Venn diagrams (RNA-seq data) of cytokines and cytokine receptor genes (in *italics*) that were downregulated (FC <0.8, left diagram) or upregulated (FC >1.2, right diagram) in IFNγ +CA-treated cells compared to IFNγ alone (D21 and T21). Cytokines with matching trends from RNA-seq (4h) and cytokine protein measurements (24h) are listed in bold, whereas cytokines with inverse trends in at least one cell type are marked with an asterisk.

Figure 5

Fig 5. Mediator kinases regulate splicing in pathway-specific ways. (A) Table of alternative exon usage from untreated T21 cells compared to D21. Inclusion criteria were assessed at FDR <0.05, | InclusionLevelDif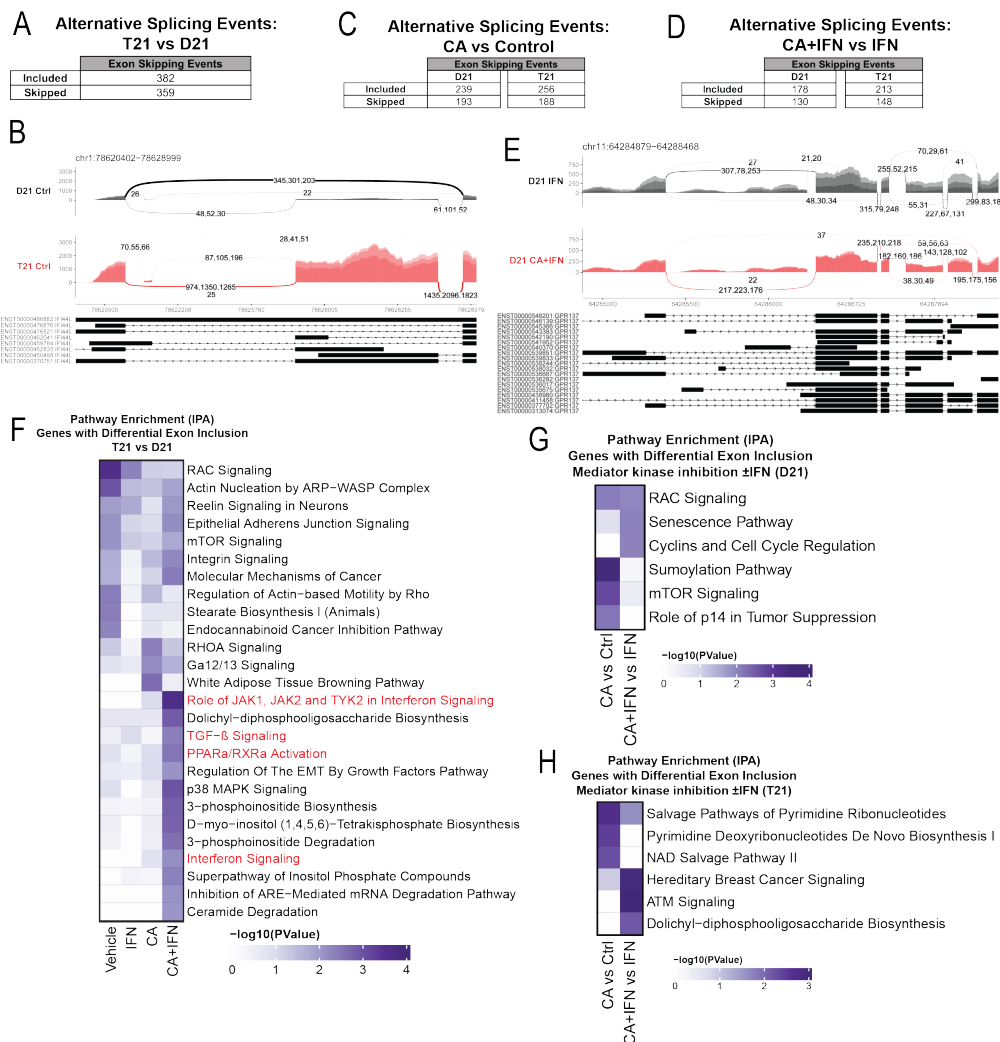ference | >0.2, and ≥2 reads/replicate. **(B)** Sashimi plots for the IFI44L gene, with normalized read numbers for D21 control (black) and T21 control (red) samples on the Y-axis, and splice junction read numbers (representing each of 3 replicate experiments) for sense strand transcripts shown in black. **(C)** Table of alternative exon usage from CA-treated D21 or T21 cells compared to controls. Inclusion criteria were an FDR <0.05, | InclusionLevelDifference | >0.2, and ≥2 reads/replicate. **(D)** Table of alternative exon usage from D21 or T21 cells treated with IFNγ and CA compared to IFNγ alone. Inclusion criteria were an FDR <0.05, | InclusionLevelDifference | >0.2, and ≥2 reads/replicate. **(E)** Sashimi plots for the GPR137 gene, with normalized read numbers for D21 IFNγ (black) and IFNγ+CA (red) samples on the Y-axis, and splice junction read numbers (representing each of 3 replicate experiments) for sense strand transcripts shown in black. Note more skipped alternative exon events in IFNγ +CA. **(F)** Ingenuity Pathway Analysis enrichment results of genes with alternative exon skipping events in T21 cells compared to D21 cells; different treatment conditions indicated at bottom. Some pathways relevant to IFNγ signaling are highlighted in red. The genes affected by alternative splicing in T21 vs. D21 cells could be grouped into several different signaling pathways (e.g. RAC, mTOR, integrin) that are important for robust immune responses (74, 75), suggesting how alternative splicing may influence inflammatory signaling in T21 cells. **(G, H)** Ingenuity Pathway Analysis enrichment results of genes with alternative exon skipping events in D21 (G) or T21 (H) cells treated with CA (±IFNγ).

A Alternative Splicing Events: T21 vs D21

Intron Retention Events	
Included	31
Skipped	17

Alt 5'ss Selection Events	
Downstream	34
Upstream	21

Alt 3'ss Selection Events	
Downstream	50
Upstream	43

Mutually Exclusive Exon Events	
More	58
Less	84

B Alternative Splicing Events: IFN vs Control

Exon Skipping Events	D21	T21
Included	163	218
Skipped	133	200

Intron Retention Events	D21	T21
Included	11	10
Skipped	11	9

Alt 5'ss Selection Events	D21	T21
Downstream	11	21
Upstream	19	20

Alt 3'ss Selection Events	D21	T21
Downstream	15	20
Upstream	19	27

Mutually Exclusive Exon Events	D21	T21
More	13	36
Less	13	34

C

D Alternative Splicing Events: CA vs Control

Intron Retention Events	D21	T21
Included	13	19
Skipped	10	10

Alt 5'ss Selection Events	D21	T21
Downstream	21	29
Upstream	23	17

Alt 3'ss Selection Events	D21	T21
Downstream	27	20
Upstream	19	25

Mutually Exclusive Exon Events	D21	T21
More	13	39
Less	23	27

E Alternative Splicing Events: CA+IFN vs IFN

Intron Retention Events	D21	T21
Included	14	7
Skipped	6	17

Alt 5'ss Selection Events	D21	T21
Downstream	9	19
Upstream	11	14

Alt 3'ss Selection Events	D21	T21
Downstream	23	31
Upstream	17	27

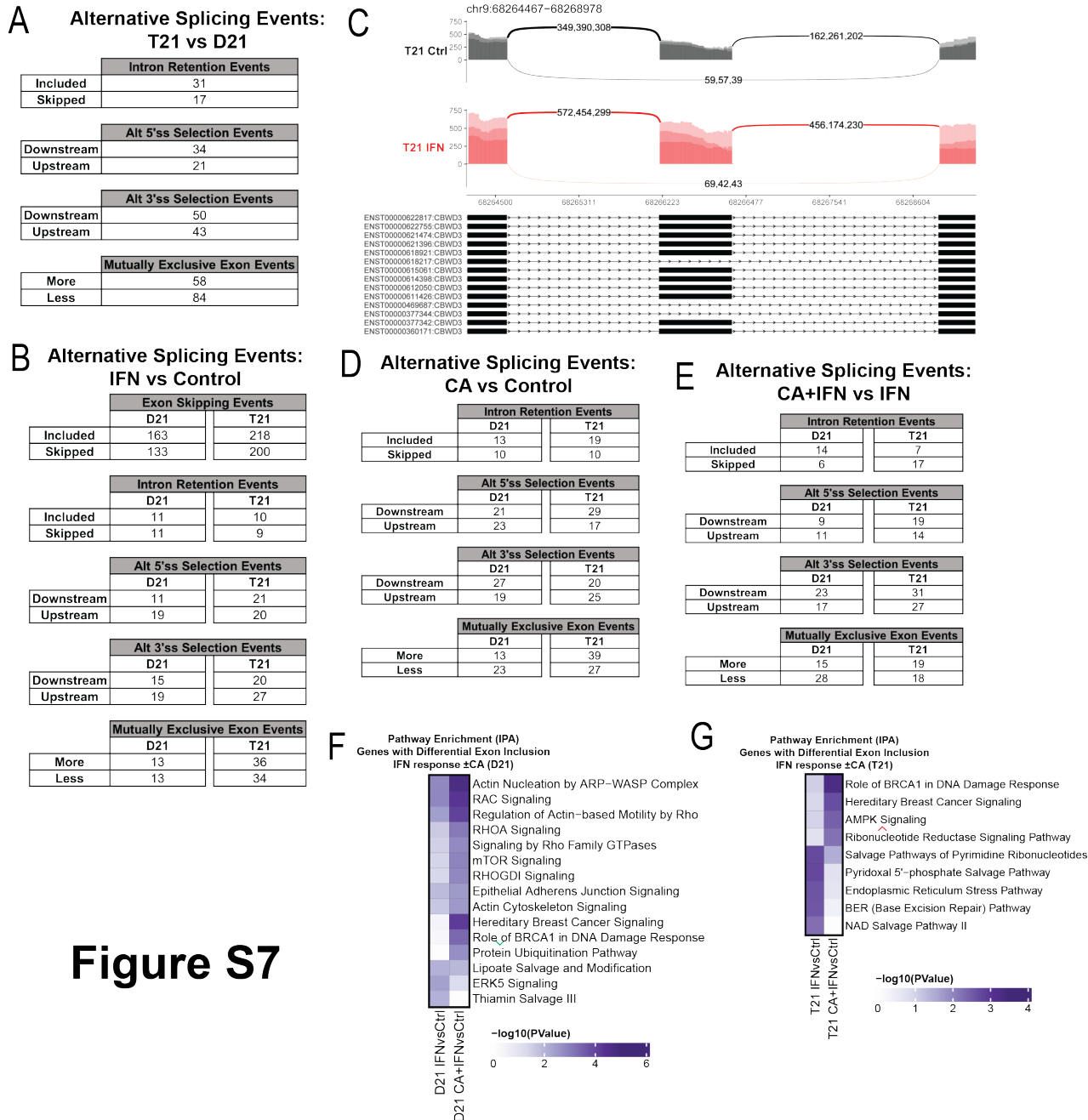| Mutually Exclusive Exon Events	D21	T21
More	15	19
Less	28	18

F

G

Figure S7

Figure S7. Additional information about splicing changes. (A) Table of alternative splicing events (RNA-seq data) from untreated T21 cells compared to D21. Inclusion criteria were an FDR <0.05, | InclusionLevelDifference | >0.2, and ≥2 reads/replicate. **(B)** Table of alternative splicing events from D21 or T21 cells treated with IFNγ compared to control cells. Inclusion criteria were as indicated in A. **(C)** Sashimi plots of the CBWD3 gene, with normalized read numbers for T21 control (black) and T21 IFNγ (red) samples on the Y-axis and splice junction read numbers (representing each of 3 replicate experiments) for sense strand transcripts shown in black. **(D)** Table of alternative splicing events from D21 or T21 cells treated with CA compared to controls. Inclusion criteria were as indicated in A. **(E)** Table of alternative splicing events from D21 or T21 cells treated with IFNγ and CA compared to IFNγ alone. Inclusion criteria were as indicated in A. **(F, G)** Ingenuity Pathway Analysis enrichment results of genes with alternative exon skipping events in D21 (F) or T21 (G) cells treated with IFNγ (±CA).
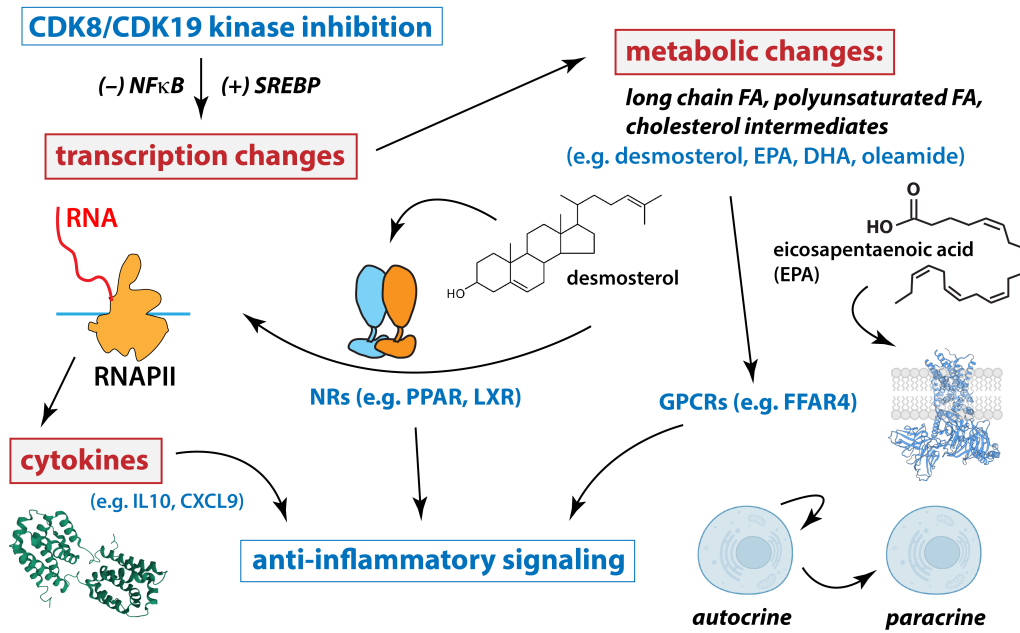
Figure 6

Fig 6. Working model for Mediator kinase-dependent suppression of IFNγ signaling.
Whereas Mediator kinase inhibition initially triggers gene expression changes that antagonize IFNγ responses, including cytokine responses, this leads to metabolic changes that can act independently to propagate anti-inflammatory signaling cascades, either through additional gene expression changes (e.g. via NR activation) or GPCR activation. Note these metabolite-driven mechanisms may act in cell autonomous or non-autonomous ways. See text for additional details.